Project Caladan

Team 21 Project Technical Report to the 2019 Spaceport America Cup

McGill University, Montreal, Quebec, Canada, H3A 0E9

Liem Dam-Quang[1], Daniil Lisus[1], Camille Richer[2,3], Nathan Robbins[3], Julien Otis-Laperrière[4], Charles Whitman[4], Zijing Yan[5], Clément Beausoleil[6], Mei Qi Tang[7], Jennie Chen[7], Raymond Yang[7], Matthew Fong[7], Luca D'Angelo[7], Jake Peters[7], and Anthony Laye[7]

[1]*Co-Captain, McGill Rocket Team*

[2]*Technical Director, McGill Rocket Team*

[3]*Aerostructures subteam, McGill Rocket Team*

[4]*Propulsion subteam, McGill Rocket Team*

[5]*Recovery subteam, McGill Rocket Team*

[6]*Payload subteam, McGill Rocket Team*

[7]*Avionics subteam, McGill Rocket Team*

This document presents the technical details of the McGill Rocket Team's (MRT) 30,000 ft COTS rocket for the 2019 SAC competition, *Caladan*. *Caladan* is MRT's third attempt at a 30,000 ft COTS rocket and features a Cesaroni O3400 motor, resin-infused composites and a sophisticated avionics suite to ensure a successful flight and easy recovery. The rocket will carry a second-generation Bacterial Collection experiment which will analyze bacteria found at high altitudes. All components have been rigorously tested to ensure flight robustness. *Caladan* is named after the ocean planet in Frank Herbert's *Dune*.

I. Introduction

The McGill Rocket Team (MRT) is making its 5th consecutive entry in the Spaceport America Cup/Intercollegiate Rocket Engineering Competition. As a result of the success at last year's competition, the MRT has enjoyed increased interest and recognition among the student body. The team has grown to include over 150 members, divided into five subteams: Aerostructures, Avionics, Propulsion, Payload and Management. *Caladan* is MRT's third attempt at a 30,000 ft COTS rocket, following the off-nominal flight of *Stella* in 2017 and the failure to recover *Stella II* in 2018. Adhering to the MRT's principle of relentless iterative improvement, project *Caladan* seeks to drastically improve the team's avionics capabilities, which has historically been the team's most pronounced weakness. Other subsystems have also undergone subtle yet substantial design revisions, resulting in a rocket that is lighter and smaller than previous designs despite having a heavier and more functional avionics bay.

Fig. 1 Exterior view of Caladan

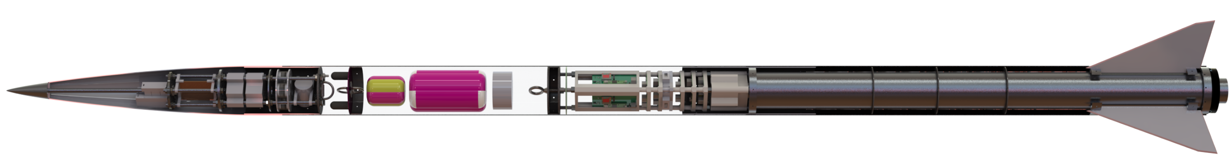

Fig. 2 Overview of internal components of Caladan

II. System Architecture Overview

Table 1 Key Technical Specifications

Specification	Value	Target	Units
Airframe Length	10.5	<11.5	feet
Airframe Outer Diameter	5.20	5.20±0.01	inches
Liftoff Mass	74.47	<75.5	lbm
Peak Thrust	1067.9	-	lbf
Max Mach Number	1.79	-	-
Motor	Cesaroni O3400	-	-
Predicted Apogee	31 880	30 000	feet
Thrust/Weight Ratio	13.5	>5	-
Rail Departure Speed	119	>100	feet/second
Minimum Static Margin	1.67	>1.5	calibers
Maximum Static Margin	6.17	-	calibers

A. Aerostructures subsystems

Caladan's airframe consists entirely of SRAD advanced composite materials. It features a Glass Fiber Reinforced Polymer (GFRP) nose cone, Glass Fiber and Carbon Fiber Reinforced Polymer (GFRP and CFRP) body tube sections and couplers, and CFRP fins. All airframe components were manufactured using our in-house Vacuum Assisted Resin Infusion Process (VARI).

The team obtained excellent results with its VARI airframe components at SAC 2018; both rockets launched remained structurally sound at all points of flight. The aerostructures division has since focused its design efforts on optimising *Caladan*'s airframe and internal structures as much as possible. These efforts have allowed for the complete removal of one body tube section, shortening the rocket by an impressive six inches. This shortening helps by reducing the mass of the airframe as well as significantly reducing the bending moments experienced by the airframe during flight and preventing over-stability.

Finally, the aerostructures division worked to improve the VARI manufacturing process by refining the vacuum bagging and infusion techniques used; significant improvements were also made in safety procedures for handling hazardous chemicals. These improvements aided in reducing the lead-time on component manufacturing and improved the safe working conditions for team members throughout the manufacturing process.

1. Overview of VARI Process

All composite components of *Caladan*'s airframe were manufactured using VARI. This advanced composite material manufacturing process was developed by the team with the intent of producing high-quality components at a fraction of the price of prepreg composite materials. In contrast with prepreg methods, VARI uses atmospheric pressure to push the liquid polymer matrix (epoxy resin) into the dry fiber reinforcement (either fiberglass or carbon fiber). There are three major steps in the VARI process: the layup, the infusion, and the cure. The layup, illustrated in the first image of Figure 3, involves setting up the dry fiber preform and consumables onto a mould (or tool). In the figure, a flat aluminum tool was used and the whole layup was placed under vacuum. The infusion consists of drawing the liquid resin through the aforementioned layup using the differential pressure between the atmosphere and the vacuum bag. The second image of Figure 3 shows the resin impregnating the part during the infusion. Finally, the last step of the process is to allow the resin to cure under vacuum, as illustrated in Figure 3.

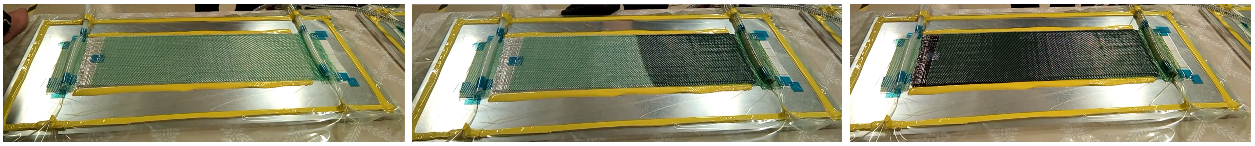

Fig. 3 Various stages of the VARI process.

Despite the excellent dimensional accuracy and material composition results obtained with the process last year, a number of minor improvements have been made to the process. First, a resin overflow has been introduced so as to further reduce the void content of the component and eliminate air-bubble concentrations present near the resin outlet. This change resulted in a much lower bubble concentration at the outlet, making possible the production of 49.5" long body tubes, 1.5" longer than those obtained in previous years. Additionally, changes were introduced to the bagging process to reinforce areas prone to leakage. This resulted in a more consistent bagging process and reduced the time necessary to fix bag leaks from an average of one and a half hours to less than one hour.

2. Moulds

The excellent tolerances and surface finishes of the team's VARI components are the result of a set of carefully designed RenShape (polyurethane) female moulds. Each mould is tailored for the VARI process, featuring O-ring slots to prevent resin seepage, dowel pin holes for mould alignment, bolt holes to fix each half of the mould, and larger diameter inlet and outlet mould surfaces. The moulds are machined on a CNC router (shown in Figure 4), sanded, coated with a polyester coating, then buffed until a smooth surface finish is achieved. The 5" moulds used during the previous year's design cycle remained in excellent condition, allowing for their reuse during the manufacturing of *Caladan*'s airframe. Figure 5 and Figure 6 show the body tube mould and the nose cone mould ready for use.

Fig. 4 Mould machining on the CNC router.

Fig. 5 Body tube mould.

Fig. 6 Nose cone mould.

The dry preform is initially put onto a mandrel, which is inserted into the mould before it is closed and the vacuum bag is applied. Once the bag is under vacuum, the fibers remain compressed against the mould surface due to atmospheric pressure, and the mandrel may be removed. After infusion and curing, the mould is easily disassembled, and a smooth external finish is left on the part due to the mould's female tool surface, as shown on Figure 7.

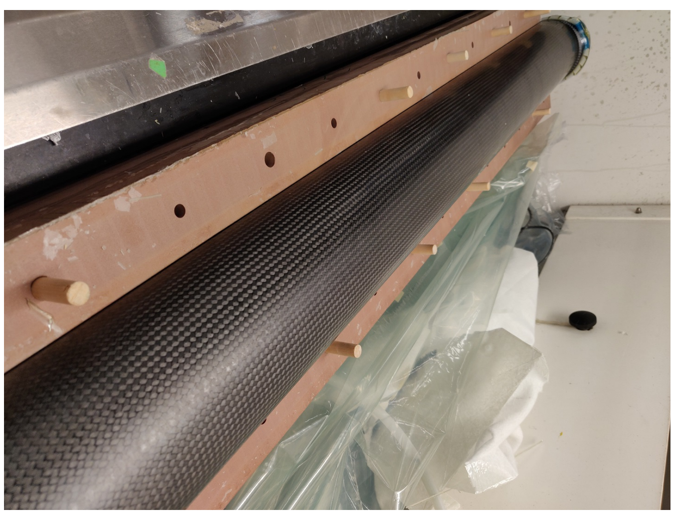

Fig. 7 CFRP Body tube during de-moulding operation.

Using this combination of female mould and mandrel, excellent dimensional accuracy can be obtained. For both the couplers and the body tubes, a range of $\pm 0.01''$ was achieved on the outer diameter. This not only good aerodynamically, as the rocket is circular, but also makes it possible to obtain a very good fit between the body tubes and the couplers, as shown in Figure 8.

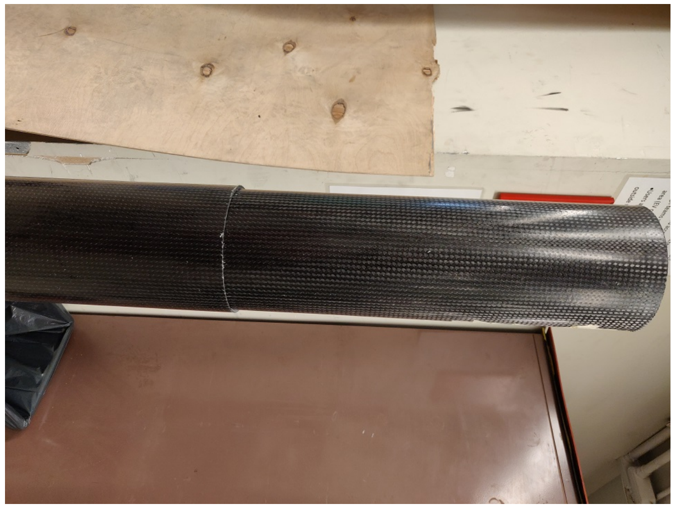

Fig. 8 CFRP body tube and coupler mating.

3. Body tubes and Couplers

The majority of the body tubes and couplers used in *Caladan* are made out of GFRP with the exception of the aftmost body tube where the motor is located and the coupler located in the nose cone, which are CFRP. Though GFRP is considerably heavier than CFRP, it allows for a lighter airframe than our previous rocket. Integration of the avionics and recovery subsystems facilitated the shortening of the entire airframe by half a foot and the removal of a coupler, contributing to the reduction of mass of the rocket. This also allows a larger window of RF-transparent rocket section, which significantly increases our capacity to maintain communication with the rocket during flight.

The CFRP body tube, in which the rocket's motor is located, features a $[\pm 28/0_2]_s$ layup. This layup provides the necessary compression strength and bending stiffness to withstand the loads experienced by the rocket during the flight, by achieving an equivalent stiffness 12.8 msi and a bending stiffness of 90.8 Glb-in. The CFRP coupler, present at the interface between the nose cone and the GFRP body tube, features a similar layup.

The GFRP body tube and coupler features a $[\pm 28_3/(0/90)_2]_T$ layup. Due to restrictions on available materials, the layup of GFRP components differs from that of CFRP components. However, this layup still achieves a very high compression strength and bending stiffness, resulting in extremely large safety factors.

Compressive testing was conducted on the CFRP body tube, in order to assess how strong the VARI components are compared to theoretical values. Under a compressive load of a little over 21 000 lbs, the body tube experienced a delamination failure. As this load is much higher than the expected aerodynamic loads, shown in Figure 9, the safety factor obtained for the CFRP body tube is extremely high. It is also suspected that the body tube is able to whistand a much larger load than what obtained in the test, due to the cuts at the edges of the body tube not being perfectly square, resulting in a reduced load bearing area.

To compute the dynamic pressure in Figure 9, the compressibility of air has to be taken into account. Assuming an isentropic flow (where skin friction does not significantly heat up the flow), the ratio of total pressure to static pressure is given by

$$\frac{P_t}{P} = \left(1 + \frac{\gamma - 1}{2} M^2\right)^{\frac{\gamma}{\gamma - 1}}$$

where P_t is the total pressure, P is static pressure, γ is the specific heat ratio and M is the Mach number [1]. Assuming that $\gamma = 1.400$, and given that $P_t = P + q_c$, the compressive dynamic pressure, q_c, is given by

$$q_c = P\left[\left(1 + 0.2M^2\right)^{\frac{7}{2}} - 1\right].$$

Note that the static pressure is determined by OpenRocket using an International Standard Atmosphere model, and values from this model are used in calculations. The drag force shown in Figure 9 is calculated directly by OpenRocket.

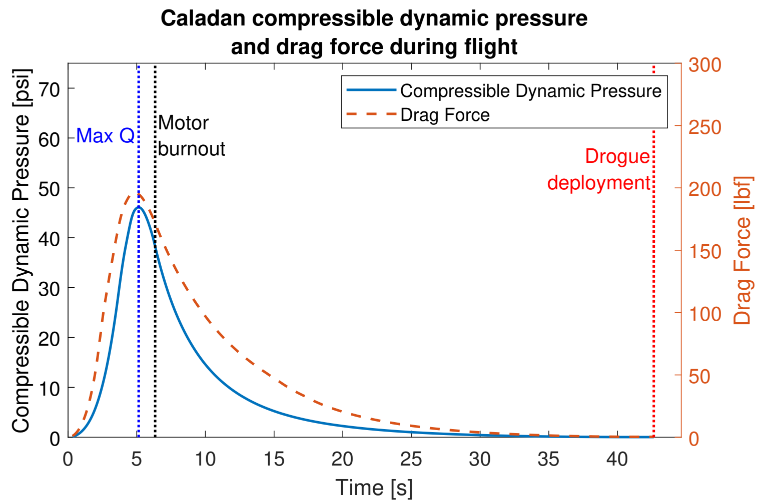

Fig. 9 Compressible dynamic pressure and drag force

Due to availability of the compression testing aparatus, it was not possible to test a sample of the GFRP body tubes. However, analysis was done to quantify the expected reduction in properties for the GFRP material. With the combination of the layup differences between the CFRP and the GFRP body tubes and the differences in material properties, reduction in compression strength of 22.6% is expected. This number was obtained by using classical laminate theory, namely the maximum stress, Hashin and Quadratic failure criteria for composites. Using this result, it is then possible to conclude that the GFRP body tubes and couplers also have a very large factor of safety for the loads experienced in flight by the airframe.

4. Nose Cone

Caladan's nose cone is made out of GFRP and features a $[(0/90)_8]_T$ layup. GFRP was selected over CFRP material since the nose cone houses the payload. The payload features an Iridium GPS module for tracking purposes and therefore requires the nose cone to be RF transparent.

The nose cone also features an aluminum tip, that allows proper integration with the payload wedding cake structure and reduces assembly time. The nose cone features a circular shoulder section that mates perfectly with the coupler and the body tube sections.

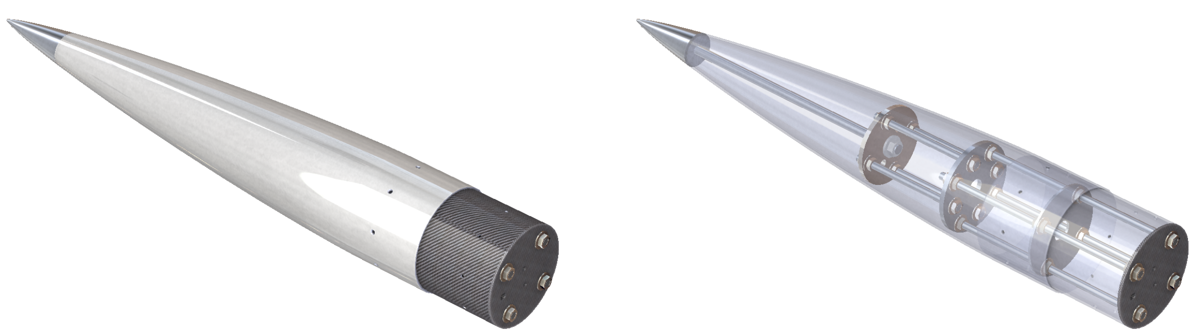

(a) von Kármán GFRP nose cone with CFRP coupler.

(b) Internal structure.

Fig. 10 *Caladan*'s Nose Cone Assembly.

A Von Kármán nose cone geometry was selected, for its excellent aerodynamic performances in the transonic regime and the supersonic regime. It also has decent performance in the subsonic flight regime, making it the optimal choice for Caladan's flight pattern.

5. Fins

Caladan features a set of three CFRP fins, fastened to the rocket using a through-the-wall attachment method. The fins utilize a quasi-isotropic layup; $[(0/90)_2/(\pm 45)_2/(0/90)]_s$, resulting in an equal stiffness in all loading directions. This is the ideal layup for fins, as it can resist both normal and torsional bending moments experienced in flight.

Caladan's fins are manufactured using a pseudo-RTM (Resin Transfer Moulding) process. Similar to VARI, RTM is a process in which the resin is pushed through a dry pre-form using a pressure differential. The main difference is that with RTM, pressure is applied on the part to obtain an extremely consistent thickness throughout. This was done using a 2-part flat tool that applies consistent pressure on both sides of the part during the infusion process. This results in a fin thickness of 0.235" ± 0.005" and two extremely smooth, blemish-free surfaces.

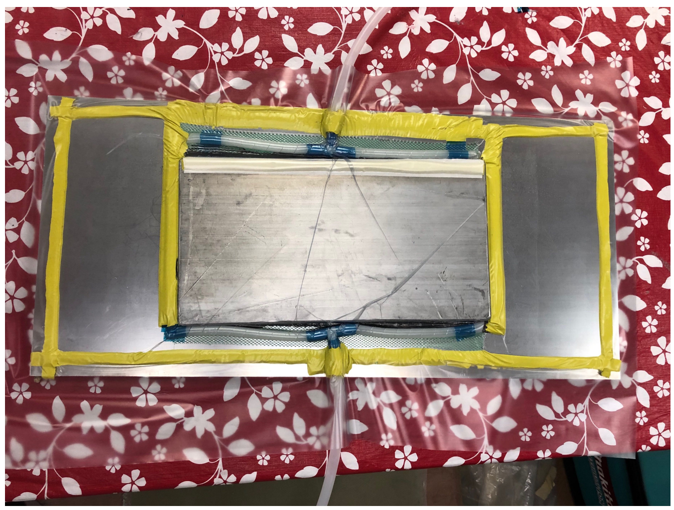

Fig. 11 Pseudo-RTM process for fin manufacturing.

The primary mode of failure of sounding rocket fins is flutter. To mitigate this, rigorous fin flutter analysis was conducted to ensure the fins do not detach from the body during flight. As with the rockets of prior years, *Caladan*'s fins have a thickness of 0.235", ensuring a high resistance to flutter. Additionally, fin flutter analysis was conducted using the *AeroFinSim* software. Using the U-G method [2], which is the most appropriate for transonic and supersonic flight, a flutter velocity of Mach 2.8 is obtained. This value is well beyond the maximum velocity reached in flight of mach 1.8, allowing a significant safety factor for fin flutter.

In addition to flutter analysis, care has also been put into properly attaching the fins to the rocket's body, to ensure that no separation occurs in flight. The fins are attached with epoxy using a through-the-wall design. Proper alignment is obtained using a Medium Density Fiberboard (MDF) jig that was machined on a CNC router. Once the fins are in place with epoxy, an epoxy clay filet is applied to the root of the fin. Finally, the fin is reinforced with carbon fiber at the root using wet-layup. This three step process ensures a precise alignment and a strong fin attachment, creating a cantilever beam fin attachment model. This method has been selected over a tip-to-tip reinforcement method, as it provides significant weight savings while still providing excellent strength. A tip-to-tip layup is also not necessary, since the fins are manufactured as a single solid CFRP component and therefore are not likely to split.

Caladan's fins also feature a double knife-edge cross-section. A Computational Fluid Dynamics (CFD) study was performed on different fin cross-section by the team in previous years [3]. This study showed that the double knife-edge results in minimal performance loses compared to an airfoil cross-section. A knife-edge cross-section is also much easier to manufacture than an airfoil, further confirming our choice.

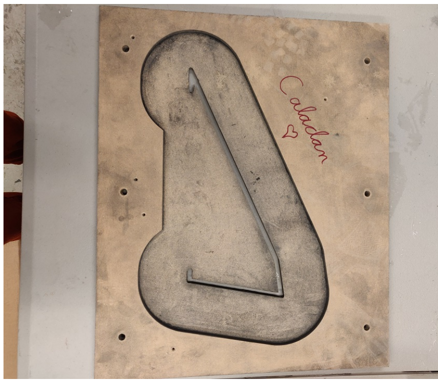

Fig. 12 MDF jig used to machine the fins.

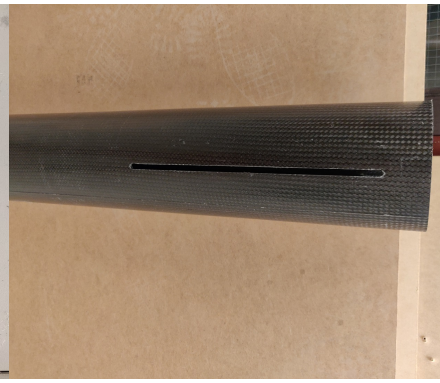

Fig. 13 Fin slits in the body tube machined using MDF jig.

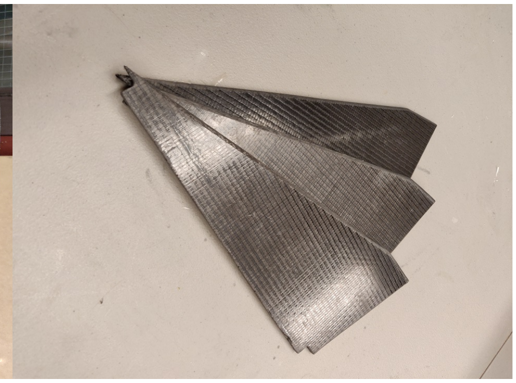

Fig. 14 Fins after machining using an MDF jig.

Finally, the fin shape for *Caladan* was carefully selected, as it plays a large role in determining the rocket's center of pressure. Using *OpenRocket* simulations, the fin shape was optimized to ensure that the rocket is stable for a wide range of wind conditions relevant to launch. An off-rail stability between 1.5 and 2.0 body calibers is obtained when simulating with wind speeds between 5 mph and 10 mph, as shown in figure 15a. A stability within this range immediately off the rail means that the rocket has a second to gain momentum before its stability increases enough to make it prone to weathercocking. This initial momentum reduces the impact of wind on the rocket's trajectory, as the weather induced wind speed is quickly dwarfed by the upward velocity of the rocket. During flight, the stability never exceeds 6.17 within this wind range.

As shown in figure 15b, the stability results match with the other flight characteristics; stability increases as *Caladan* breaks the sound barrier, due to the increased air pressure on the fins, which causes the CP to move aftward. Stability is minimum when the rocket is at its maximum supersonic speed. As *Caladan* slows down after motor burnout, stability again increases to a maximum of 6.17, higher than previously as the motor is fully burnt. The oscillations at the end of the ascent are due to wind turbulence in the simulated atmosphere.

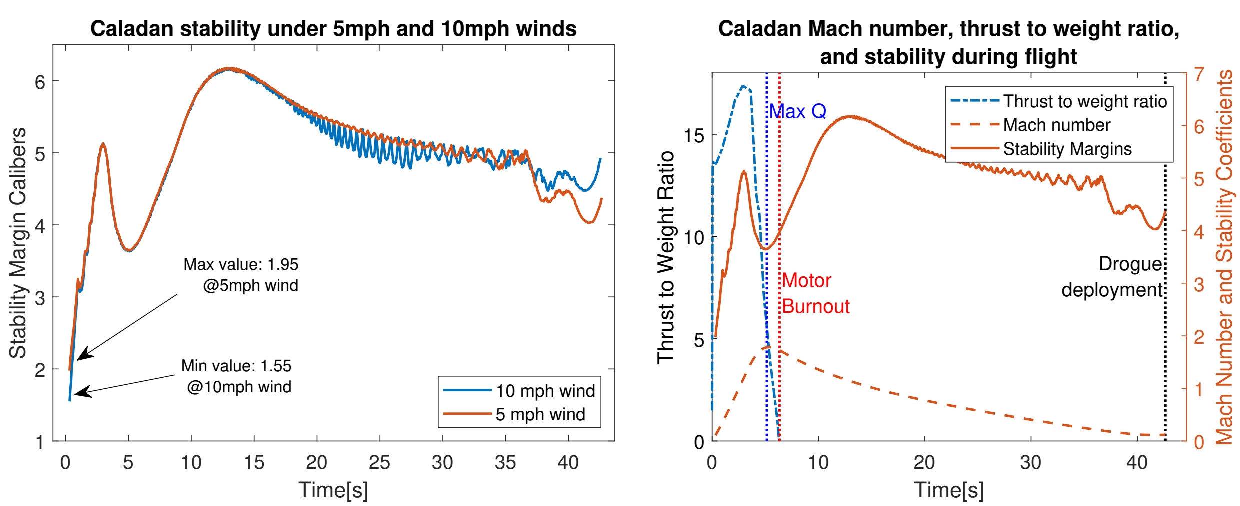

(a) Comparison of rocket stability at 5mph wind and 10mph wind.

(b) Flight Dimensionless Coefficients.

Fig. 15 *Caladan*'s Ascent Behavior.

6. Systems Integration

In comparison with last year's rocket, *Caladan*'s internal structure allows for superior systems integration lessening wasted internal space. This was achieved by the addition of a structural attachment point in the centre of the GFRP body tube section. This attachment point allows the recovery bay and the avionics bay to be contained within the same body tube section, eliminating the need for an additional coupler and body tube section. This also results in a weight reduction of the airframe of about 1 lb. In last year's rocket, a total of three body tubes sections and three couplers were used. In *Caladan*, a total of two body tube sections and two couplers are used. Figure 16 shows a comparison of Caladan's airframe and last year's rocket Stella II.

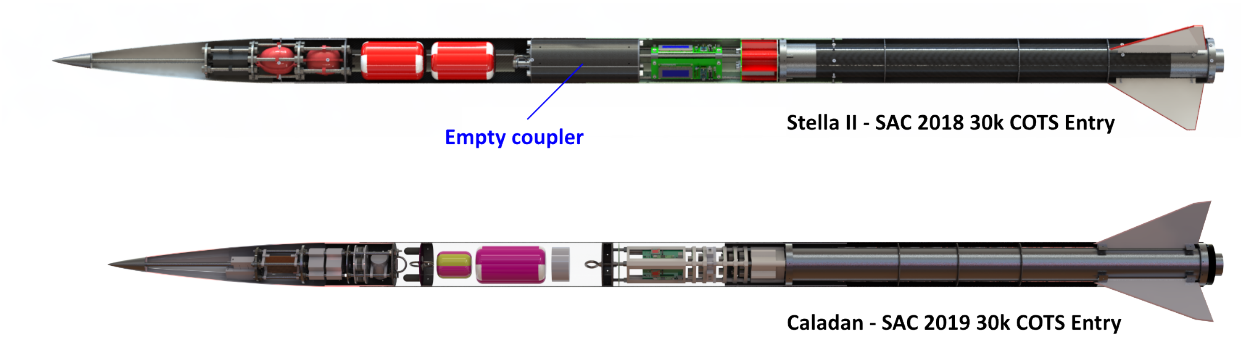

Fig. 16 Side-by-side comparison of 2019 and 2018 entries

B. Recovery Subsystems

The internal structures and recovery systems were designed with the main objective of minimizing weight and volume without compromising reliability. The team opted for a single separation and dual deployment recovery sequence (see Figure 17), a setup which has been successfully implemented in previous projects. Separation and drogue deployment occur at apogee, at the nose cone connection. The main deployment is set to occur at 1500 ft.

Fig. 17 Deployment Sequence.

1. Internal Structures

In this year's rocket, coupler rings, which are essentially inch-long couplers, were integrated into the internal structure to serve as stoppers for bulk plates. These rings allow the creation of separate chambers within a single body tube. In doing so, the avionics, recovery, and ejection bays may be kept inside a single body tube, whereas in previous years' rockets, they were kept in two different tubes. Therefore, with the current design, one less coupler is needed, resulting in weight savings of approximately one pound and in a simpler and quicker assembly at competition. Additionally, thin plastic straws are epoxied on the inside wall of the body tube to guide wires during assembly. The straws also serve as a sheath to protect the wires from getting damaged during the packing of recovery components, which often fit tightly inside the tube.

2. Ejection Mechanism

Due to weight considerations, the team has chosen to use traditional chamber pressurization with the combustion of black powder, which is the lightest and typically the most reliable ejection method. However, there are concerns about the lack of air as a medium for heat transfer at higher altitudes, as it may result in an incomplete combustion of the black powder due to premature dispersion. Therefore, the charge wells are made of aluminum and designed to be slim and long enough so that black powder particles may be held close together for as long as possible once combustion begins. The charge wells are also sealed with a silicone cap secured with silicone tape for additional containment, as shown in Figure 18.

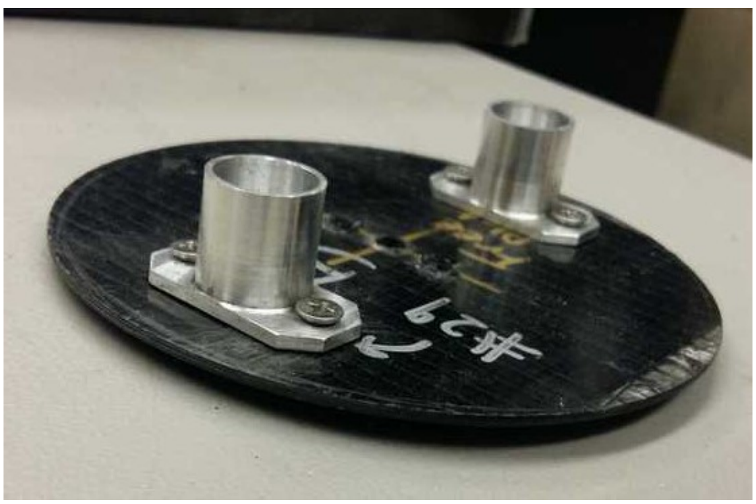

Fig. 18 Charge Wells and Rubber Caps.

To ensure that the nose cone stays attached to the main body tube during ascent, eight 4-40 nylon screws are used to overcome the pressure differential with a safety factor of 3.1. At apogee, the ejection chamber is designed to be pressurized by the combustion of black powder until the nylon screws break to allow the nose cone to separate. Each charge well contains 1.4 grams of FFFF black powder, which is able to break all the nylon screws with a safety factor of 2.2. For redundancy, two separately-wired charge wells are used.

To further ensure full combustion of the black powder, the ejection chamber is designed to be as small as possible in order to minimize the amount of powder needed. As shown in Figure 19, the top of the chamber is confined by the bulk plate connected to the nose cone. The bottom side of the chamber is quarantined by another bulk plate, which simply rests against a small coupler ring which is screwed into the airframe. This plate, which houses the two charge wells, serves to enclose the ejection chamber, while protecting the parachutes located right below it from the blast. Once the nose cone is ejected, the plate is pulled out of the tube (note that the plate eye bolt is connected to the nose cone bulk plate via a shock cord), allowing the drogue parachute to deploy. The plate and coupler ring system has been ground-tested multiple times (see Figure 20).

Fig. 19 **Ejection Chamber with Stopper Ring and Free Plate.**

Fig. 20 **Ejection Testing.**

3. Parachute Deployment

The drogue parachute freely deploys as a result of the separation at 30,000 ft. At separation, the main parachute remains packed and held inside the body tube by pyrotechnic links known as tender descenders (see Figure 21). The tender descenders have been tested and performed impeccably in previous projects, so the design remains unchanged. One tender descender contains 0.08 grams of FFFF black powder, which can cause separation with a safety factor of 3.4. Two tender descenders are connected in series for redundancy. At 1500 ft, the tender descenders separate, allowing the drogue parachute to pull on and deploy the main parachute.

(a) Assembled.

(b) Tested.

Fig. 21 Tender Descenders.

The drogue parachute is folded and wrapped with a flat piece of that fabric so that it can freely deploy, while the main parachute is contained within a deployment bag. The bag is in a cylindrical shape with a diameter slightly smaller than that of the body tube so that it can slide out smoothly. Rows of sectioned elastic bands are integrated into the bag, so that shroud lines may be packed and secured for a controlled deployment. Due to the extensive use of black powder in the rocket, precautions are taken to protect the parachutes from the blasts: deployment bags, blankets, and tender descender protective sheaths are all made of a fire-retardant fabric composed of a Nomex and Kevlar blend.

4. Parachute Design

The main parachute is designed and manufactured with a pull-down apex (see Figure 22), which provides a drag coefficient estimated at around 2.2, as opposed to classic semi-elliptical parachutes which the team has made in the past, where the drag coefficient is experimentally determined to be closer to 1.6. The pull-down apex design therefore allows for smaller diameter parachutes for a desired descent speed, resulting in smaller packing volumes. However, since the pull-down apex design typically involve higher opening speeds than those in classic semi-ellipsoidal ones, the parachute opening shock force will be higher. From calculations and simulations using *Oscalc*, the drogue parachute may experience up to 1400 lbs of force due to the separation event at apogee, while the main parachute should only experience up to 500 lbs of force. Thus, the pull-down apex design is only implemented for the main parachute, while the drogue parachute remains semi-ellipsoidal. This decision is also justified by the fact that the drogue parachute is too small for any packing volume savings to be significant enough. Both the drogue and main parachutes' specifications are listed in Table 2.

Fig. 22 Pull-Down Apex Parachute.

Table 2 Parachute Specifications

	Drogue (2018)	**Drogue (2019)**	**Main (2018)**	**Main (2019)**
Shape	Semi-ellipsoidal	Semi-ellipsoidal	Semi-ellipsoidal	Pull-down apex
Drag coefficient	1.65	1.65	1.65	2.2
Diameter	24	20	108	84
Number of gores	8	8	12	12
Terminal speed (ft/s)	93	115	21	22

All gores are stitched together using a flat-felled seam, which is one of the strongest and neatest seams available. Shroud lines are triple-stitched to the canopy with grosgrain ribbon. The parts of the parachute which undergo the largest amount of stress, the vent hole and the shroud line attachment points, are further reinforced using bias tape and bar tacks respectively. All stitching is done using coated nylon thread. The canopy fabric is composed of 1.1 oz zero-porosity rip stop nylon, in order to maximize drag. The shroud line strength for each parachute are chosen based on the forces they are expected to undergo. Each parachute is attached to a swivel joint to prevent line tangling.

5. Recovery Harness

In the past, the team's recovery harness, which includes quick links, eye bolts, shock cords and parachutes, were designed as a whole to sustain a certain amount of force. However, different components in the harness do not undergo the same stresses, some of them became over-designed, resulting in unnecessary bulk and weight. This year, each recovery harness component is individually designed, selected, and manufactured as to reduce packing volume and weight, while maintaining a safety factor around 2, as to not have one weak link in the chain that defines the strength of the entire harness. For instance, the main parachute's shroud lines were switched from 400-lb break nylon to 100-lb break nylon, which reduces the packing volume by almost half, while still providing a safety factor of 3.2. The shock cords were also switched from 1" tubular nylon webbing to both 5/8" and ½" tubular nylon webbing. Table 3 summarizes all the recovery harness components and their respective strengths and safety factors. Additionally, shock cords were directly sewn onto eye bolts and parachute swivels as to reduce concentrated stresses at metal-to-metal connection points with quick links, and also as to decrease the number of quick links needed, which in turn reduces weight and facilitates assembly. These design changes allowed the packing volume and weight of the recovery components to be reduced by approximately 25%.

Table 3 Recovery Harness Components Strength

Deployment	**Component**	**Strength (lbs)**	**Factor of Safety**
Drogue	Drogue parachute	3000	2.1
Drogue	Shock cords (5/8")	2900	2.1
Drogue	Quick links, eye bolts	3000	2.1
Main	Main parachute	1600	3.2
Main	Shock cords (1/2")	990	2.0

C. Avionics subsystems

Caladan's avionics have received significant upgrades when compared to previous iterations, in part due to an increase in the subteam's size and to the increased investment of resources in research and development. Significant improvements include a refined avionics bay structure design, a novel power management system for providing all SRAD circuits with a stable voltage source throughout the flight, the use of patch antennae in radio communications, an improved ground-station software, and the development of adequate equipment for surface mounted device (SMD) reflow soldering.

Furthermore, the subteam has expanded its knowledge base on antenna theory and design. Access to an anechoic chamber, as seen in Figure 23, has been crucial in the development and performance of tests for characterizing antennae and radio modules. By re-evaluating the hardware used in the previous design year, the team is able to determine their shortcomings and improve on the design for *Caladan*. The new implementation employs radio modules with higher transmitting power and optimized configuration settings, patch antennae for transmitting telemetry data from the rocket, and receiver Yagi antennae - shown in Figures 24 and 25. Through these hardware replacements, we are able to increase the data transmission range of the rocket's radio systems significantly.

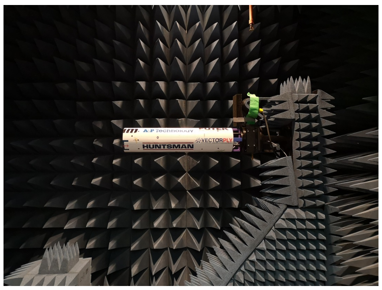

Fig. 23 Antenna radiation pattern test setup in anechoic chamber.

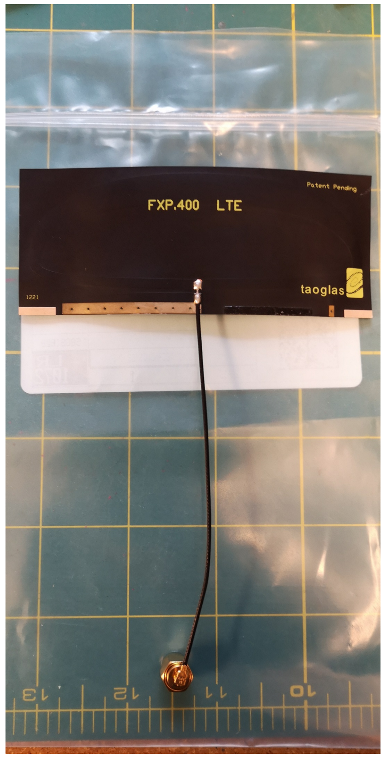

Fig. 24 One of the two patch antennae used for transmission.

Fig. 25 11.5 dBi Yagi antenna for the COTS board.

Finally, the avionics subteam has improved on the quality of its printed circuit boards (PCBs) through better design and soldering techniques. Indeed, the PCBs of every subsystem were conceptualized using *Altium Designer*, a professional and industry standard software. Stencils were also used to facilitate the application of solder paste for SMD components, the result of which can be seen in Figure 26. Lastly, to expedite the manufacturing process, a toaster oven was modified, Figure 27, to allow SMD components to reflow onto the PCBs. As a result of these improvements, the subteam was able to create and test prototype iterations in an accelerated pace.

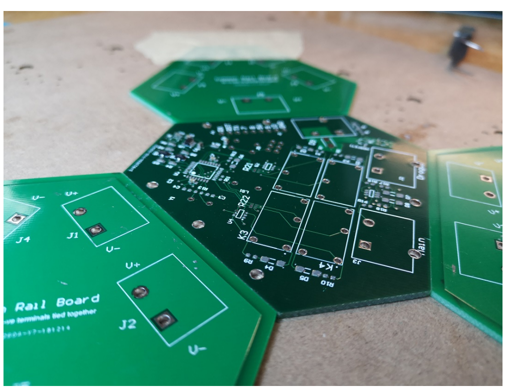

Fig. 26 PCB with solder paste applied after the stenciling process.

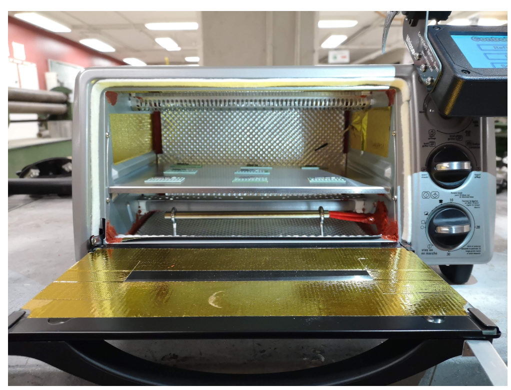

Fig. 27 Modified toaster oven used as a PCB reflow oven.

1. Structure

The avionics bay structure of *Caladan* is one of the most substantial redesigns from previous years. With a robust, vibration-reducing structure, the main motivation behind this revision is to rectify a critical oversight of past designs. Indeed, during Spaceport America Cup 2018, the cause of the communication loss with *Stella II* can be traced back to the instability of its avionics bay. The structure was solely composed of three nylons rods on top of which PCBs were attached via P-clamps, resulting in a highly flexible structure that is vulnerable to intense vibrations. In the current design, it is replaced by successive brace structures, printed out of Polyethylene Terephthalate Glycol (PETG) for its superior glass transition point as compared to other available printing materials. Figure 28 shows the final assembly of this brace structure, as each brace leg fits into a small counterbore in the next brace. The entire structure is then slid onto three nylon rods and held in compression against the top engine block by a set of nuts. The nylon rods are then fixed to an intermediate bulk plate at the top of the structure, to fix it at each end. A disassembled drawing of the structure can be found in Appendix 6: Engineering Drawings.

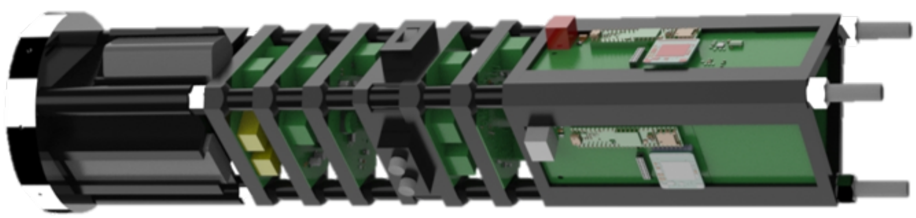

Fig. 28 Assembled Avionics Bay structure; bottom on left-hand side.

The avionics bay structure features three main sections: the battery casing at the base, a set of horizontal braces in the middle, and a vertical brace at the top. The horizontal braces are used to secure and house electronic components and PCBs that do not have any physical orientation requirements, such as the power management and ejection circuits. PCBs are attached to the horizontal braces via RTV Silicone adhesive. An intermediate brace in the horizontal section is used to mount the push and rocker switches for the arming of the electrical circuits. These switches can be manually activated with a rod through small access holes on the side of the airframe. In addition to horizontal braces, there are vertical braces used for components that require vertical orientation such as antennae. For these braces, the PCBs are mounted by sliding them into slits in the brace legs, then held in place by compression upon closing the brace structure.

2. SRAD Telemetry

Caladan's telemetry is implemented through two independent circuits: the main telemetry circuit and the GPS redundancy circuit, each connected to a separate patch antenna to transmit data. Both processes capture relevant data through their sensors, then parse this information using a microcontroller into strings of characters to be transmitted to the ground station. In the case of the main telemetry subsystem, the main microcontroller (Teensy 3.6) takes its input from 3 different peripheral modules: a digital pressure sensor (BMP280), a 9-degree of freedom inertial measurement unit (BNO055), and a GPS (Adafruit Ultimate GPS breakout module, built around the MTK3339). The information extracted from these sensors and sent to ground-station include, in order: GPS latitude and longitude, altitude, acceleration, velocity, temperature within the avionics bay, angular position and the time elapsed since the electronics were activated. As a fail-safe to transmission failure, this data is also stored locally on an SD card. Furthermore, the main microcontroller interfaces with its transmitter, a Digi XTend 900 MHz Long-Range radio frequency (RF) module. The transmitter is shielded with a copper box, where a piece of RF-absorbing material is inserted underneath the shielding and above the transmitter. The final assembled SRAD main telemetry board is shown in Figure 29 without its shielding. In the case of the GPS redundancy subsystem, it is identical to the main telemetry, but it only incorporates the GPS module as a sensor. The purpose of this setup is to provide the ground-station with backup GPS data in the case of transmission failure from the main telemetry subsystem. The GPS redundancy board is shown in Figure 30. Furthermore, a beacon mode is implemented by both processes; Once landing is detected, the radio modules will transmit at a lower frequency to save power, allowing for a longer recovery window.

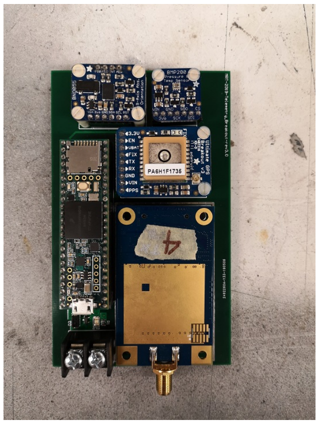

Fig. 29 SRAD telemetry board.

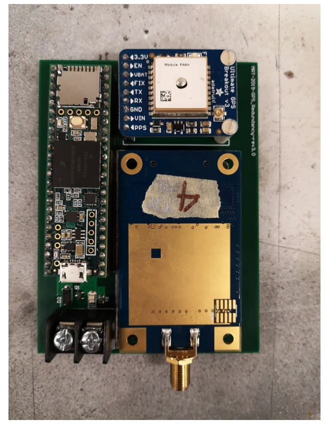

Fig. 30 GPS redundancy board.

3. COTS Telemetry

Caladan's COTS telemetry and ejection mechanism uses the Entacore Electronics AIM XTRA, seen in Figure 31. Since this board is meant to be a redundancy, it is powered by its own LiPo battery, independent from the power management circuit. The team tested two possible options for COTS boards, the AIM XTRA and the Altus Metrum Telemega. Both were subject to an outdoor Received Signal Strength Indicator (RSSI) test. For this test, we recorded the RSSI value measured by the respective receiver for each of the COTS boards. RF attenuators were added in increments of 5 dB until the receiver is no longer able to receive packets correctly from the transmitter. Our test concluded that the AIM XTRA had a better performance, hence why we chose it for *Caladan*.

Fig. 31 The AIM XTRA COTS board.

4. Ejection

The ejection subsystem's assembled PCB can be seen in Figure 32. Activation of the e-matches used for drogue and main parachute deployment is initiated by the microcontroller through means of activating four mechanical relays, each e-match is connected in series with two relays necessitating two activation signals for the detonation of the ejection charges. An ATMEGA328P-AU chip is interfaces with a BOSCH BME280 pressure sensor which continuously monitor barometric pressure and temperature readings. A control loop is implemented on the microcontroller which determines the timing of the drogue and main deployment events. When drogue deployment is to be initiated, two of the mechanical relays connected in series are triggered to open by the microcontroller and connect the e-match to a 5V source. An identical process occurs for main deployment with the other pair of relays. A continuity check is implemented on the PCB with LEDs providing visual confirmation that the e-matches are properly connected to the ejection channels.

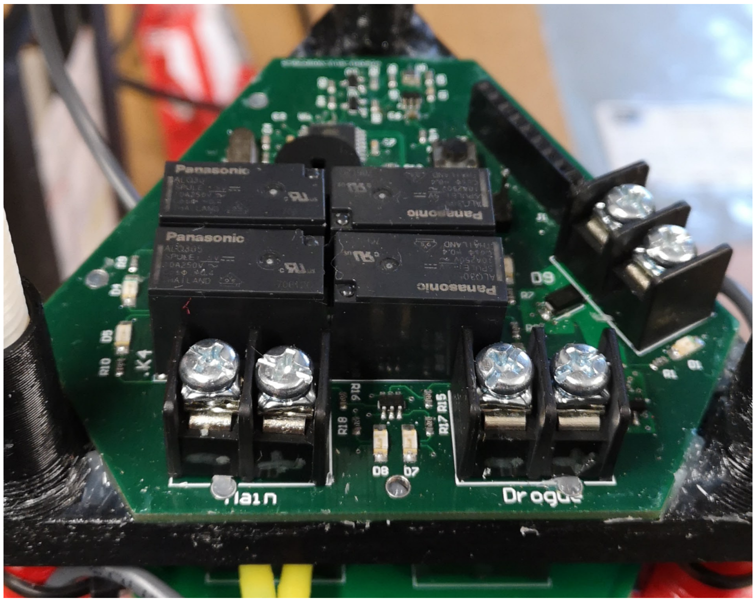

Fig. 32 Assembled ejection PCB within avionics bay structure.

5. Power Management

The power management subsystem, as seen in Figure 33, incorporates three major features: fusing and reverse polarity protection, N+1 redundancy and a high efficiency DC-DC switch mode step down power supply. Reverse polarity protection is accomplished using a P-MOSFET which blocks current flow if the ground terminal is brought to a higher voltage than that of the positive terminal, a fast blow fuse is added to protect the system from sourcing too much current from the batteries in the event of a short circuit developing downstream. The power management system is fully redundant such that if one were to fail, the other would be able to provide for the full power needs of the avionics package. The combination is accomplished using a N+1 ORing diode controller, which prevents reverse current into either power supply. The avionics package is powered by two 11.1V lithium ion batteries providing a total of 77.8Wh in capacity; a switch mode power supply is used in order to efficiently step down the voltage to the 5V required by the avionics package. A switch mode power supply was used as it provides a 85% conversion efficiency as opposed to a 45% efficiency provided by linear voltage regulators, although special care had to be taken in designing the supply to reduce ripple in the output voltage.

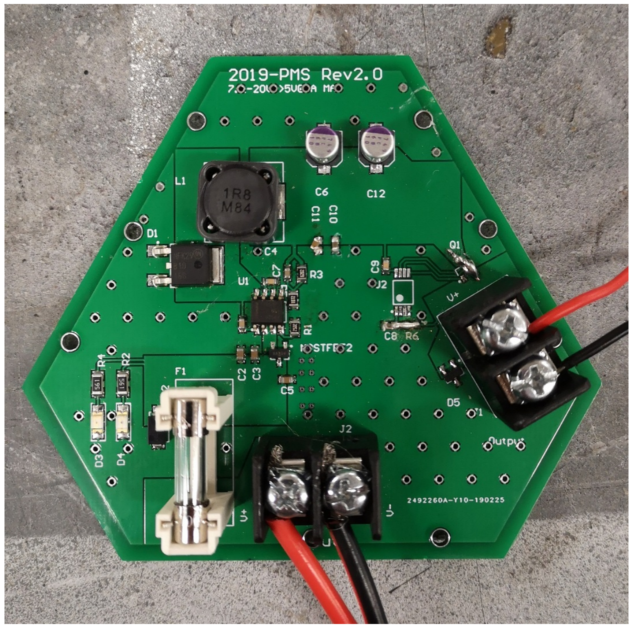

Fig. 33 Assembled power management PCB.

6. Ground-Station

The ground-station subsystem saves and plots flight data in real-time, in order to track the position of the rocket and estimate performance. The software, which can be run on any laptop, is programmed in Python. It displays performance indicators from the flight to the user using the PyQT user interface toolkit.

The user interface displays five key graphs: temperature (°C), altitude (m), velocity (m/s), acceleration (m/s^2), and GPS location (latitude vs. longitude). Flight data from the rocket is read as a string of characters from the receiver attached the the ground station; the character ‘E’ is used as a delimiter to signify the end of a transmission string. All incoming data is immediately saved to a log file to ensure everything received is recorded. The strings are then parsed by first splitting on the ‘,’ character, then attempting to convert the result into floating point values. The valid parsed values are then saved, and plotted.

At each receiver radio module, a low-pass filter is used to convert the RSSI, output by the receiver through a digital PWM signal, into an analog value. This value is read by a microcontroller, which then acts as a USB peripheral device that the ground station polls to read the signal strength of each incoming message.

Although all flight data is displayed on the graphical user interface, it is also saved to the file system on the ground station. These files, organized by date and time, ensure that all received information is stored and accessible for future analysis. This is essential because it offers the possibility to look back at previous launches or test runs to evaluate the performance of the rocket, and increases possibility for improvements. After the flight, the ground station also has the ability to re-graph files of previous flight data for analysis.

To obtain the best signal strength from the telemetry circuits, the antennas on the ground station must be pointed toward the rocket during flight. As the rocket’s height increases, it becomes harder and harder to track its approximate location with the naked eye. Since the latitude, longitude, and altitude of the ground station are known, and since the latitude, longitude, and altitude of the rocket are obtained, the relative angle of the rocket to the ground station in the xy and z-plane can be calculated. These values are displayed on the GUI and can be used to direct the antennas in the proper direction.

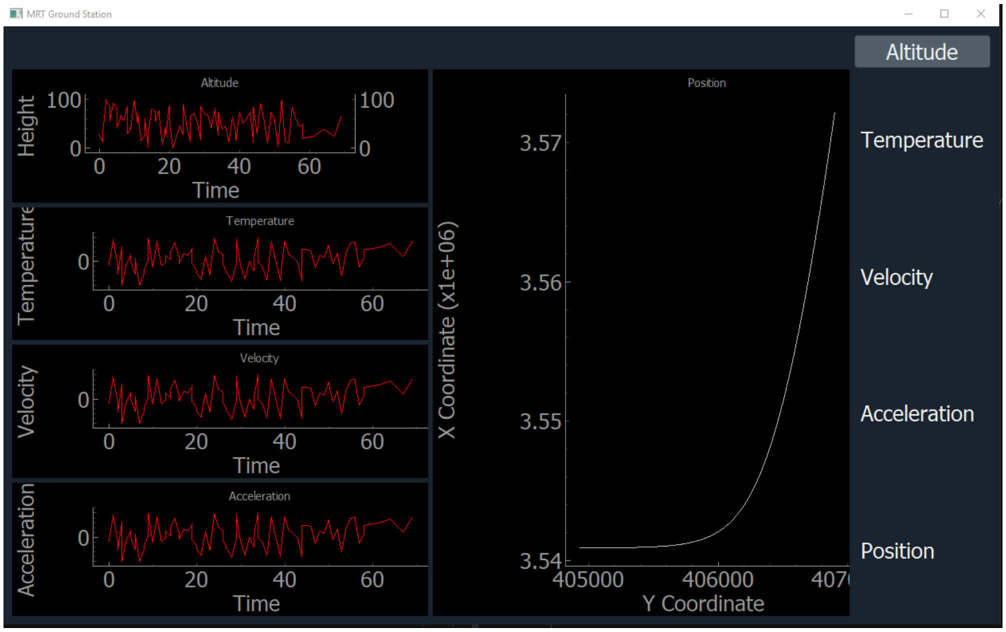

Fig. 34 Ground Station GUI

7. Testing

A critical part of the improvements made to the avionics system this year came from developing and implementing standard testing procedures for our antennae and radio modules. Their purpose is to guide our design process when choosing appropriate antennae, radio modules, and their placement within the rocket. The tests are divided into two different categories: configuration testing and integration testing.

Configuration tests took place inside an anechoic chamber. In this process, the effects of carbon fibre and glass fibre materials on patch antennae are determined and analyzed. Preliminary test setup can be seen in Figure 35. The antenna orientation and distance from the carbon fiber material are studied in order to determine the best location for the patch antenna within the rocket. With these results, obtained from initial testing, the optimal patch antenna configuration is chosen, and an antenna radiation pattern test using NSI-MI Technologies Near-Field test equipment is conducted. Figure 36 shows the resulting radiation pattern of our patch antenna. This second test, which produces more accurate results, helps in understanding the behaviour of the antenna signal throughout the flight.

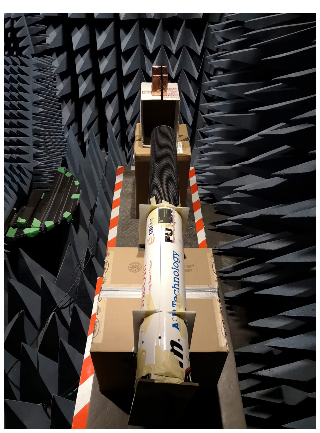

Fig. 35 Test setup for carbon fiber effects on antenna signal strength.

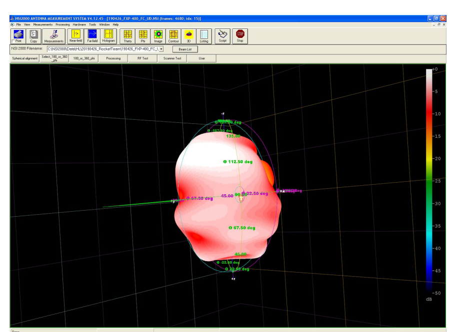

Fig. 36 Radiation pattern test result.

Integration testing aids in determining the reliability of our committed design choices under real flight conditions where different subsystems may interfere with each other's performance, especially in communication. By performing spectrum analysis and measuring the magnitude power level of an input signal over a certain frequency, potential interference effects between neighboring radio modules are detected. Figure 37 shows the result of intermodulation. Another preliminary test consists of adding RF attenuators on the receiver radio and measuring the RSSI value at close range. Subsequently, to stimulate accurate flight conditions, outdoor long range tests are conducted at 10km and 15km to mimic the approximate apogee range and recovery distances, respectively. Figure 38 shows the long-distance range test setup, where the signal strength, throughput, and interference are measured. Finally, a spin test, as seen in Figure 39, is also performed to account for the effects of the rocket's rotation about its primary axis on the signal received by the ground-station.

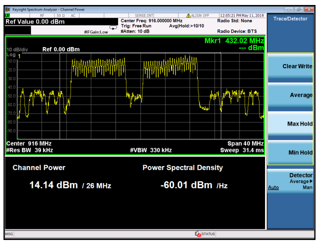

Fig. 37 Spectrum analyzer test showing the effects of intermodulation.

Fig. 38 Long range test setup.

Fig. 39 Preliminary spin test setup.

D. Propulsion subsystems

1. Engine Specifications

Much of *Caladan*'s design was determined by the motors available for use. *Caladan* employs a Cesaroni Pro98 O3400-P, the most powerful motor available to the team at the Spaceport America Cup, with a total impulse of 21,062 Ns over 6.16s and a peak thrust of 4750 N, with the full thrust curve shown in Figure 40.

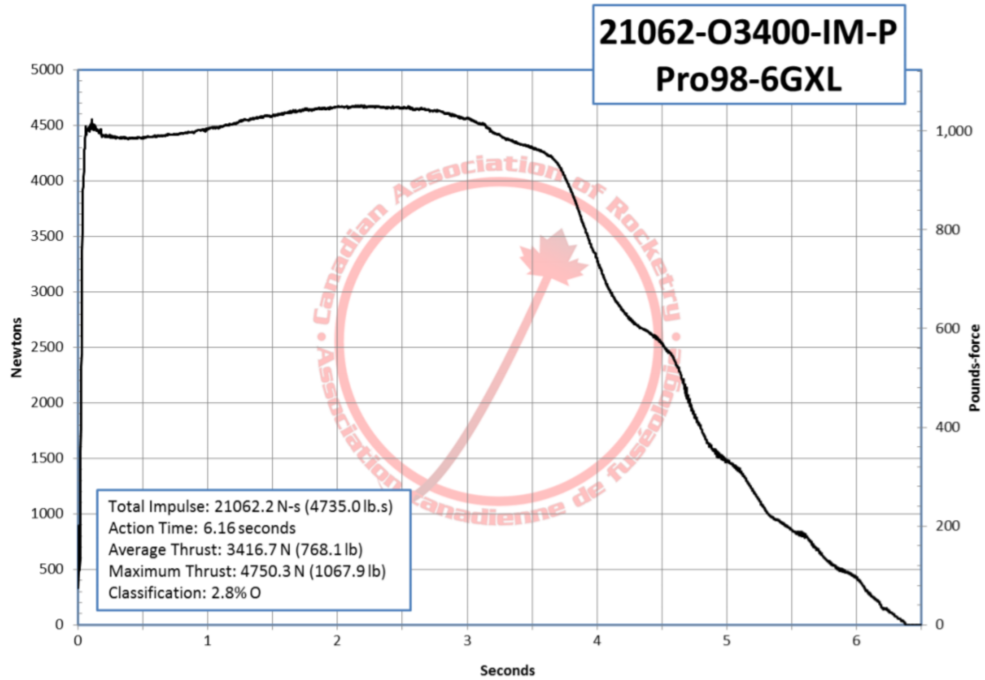

Fig. 40 Thrust curve of Cesaroni O3400 motor.

2. Engine Block

The large force applied to the airframe from the motor requires the use of carefully designed engine blocks. These prevent the motor from ripping through the rocket during peak thrust. *Caladan*'s engine block features a top and bottom component placed in indeterminate static equilibrium. The bottom piece acts as a mounting point for the retaining ring, while the top is a mounting point for the avionics. Each block is manufactured from Aluminum 6061-T6, with a yield stress of 40 ksi. While the design of the motor retaining blocks remained very similar to that of previous years, some noteworthy changes were made.

The most significant change is the placement of radially tapped holes about the bottom block. The team's 2018 bottom block design was composed of eight equally spaced holes, making the symmetric placement of screws through the body tube and into this block impossible between three fins. As a consequence, some of the tapped holes were completely obstructed by the fins. This year, the bottom block is machined with a total of nine radially tapped holes, placed in clusters of three, so as to allow for even placement between the fins. While the load from the motor is shared between the two plates, each was designed to independently withstand peak thrust, should the other fail. The top block was found to have a safety factor of 1.5 while the bottom block had a safety factor of 11. Figure 41 shows the results of the Finite Element Analysis done through the ANSYS Static Structural module, assuming worst-case loading scenarios.

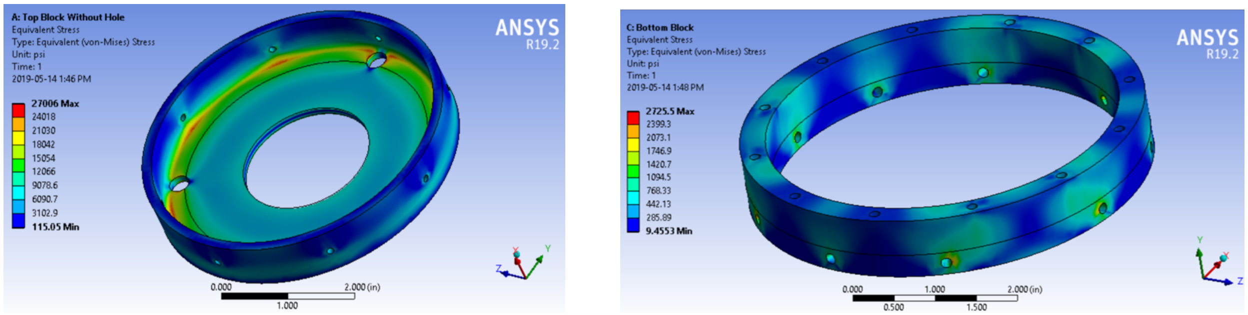

(a) Top Engine Block.

(b) Bottom Engine Block.

Fig. 41 Caladan engine blocks under worst-case loading.

3. Simulations and alternative motors

Although the engine choice was ultimately the same as *Stella II* in the previous year, several simulations were run using *OpenRocket* in an attempt to find possible alternatives. The most interesting alternative was the Cesaroni N5800, which was found to result in a slightly higher apogee despite a lower total impulse due to its very fast acceleration. However, this option was ultimately discarded due to the acceleration placing too much stress on the structural components.

Several different scenarios were considered for the simulation parameters. As mentioned in section II.A.5, stability was assessed in low wind (5 mph), medium wind (7 mph) and high wind (10 mph). These values were based off of historical weather data in the Truth or Consequences, NM region [4]. As *OpenRocket* simulation runs are randomized to account for variations in wind, each run is slightly different. For each scenario, the simulation was repeated at least 3 times to ensure the flights were not unusually stable (or unstable). round level altitude was set to 4600 ft, and the launch rail was set to a length of 17 ft at an angle of 6° from vertical.

E. Payload subsystem

Caladan's payload, the Atmospheric Microorganism Sampling Experiment (AMOSE), is a high-altitude microorganism collection and analysis experiment. In concept, AMOSE is similar to last year's SPORE payload, though another year of design allowed for improvements on several fronts; notably a sturdier housing, an improved collection method and a more comprehensive analysis. The experiment has also been modified to be non-deployable and to operate at 30,000 ft. To ensure optimal usage of space, the payload is contained inside the nose cone of *Caladan*.

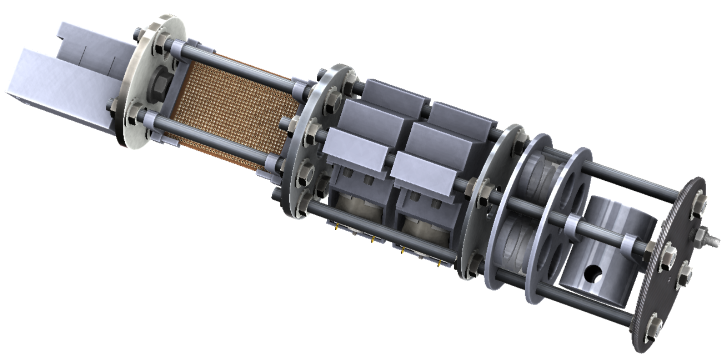

Fig. 42 Assembled Payload Structure.

In light the structural failure of our semi-deployable housing last year, which led to the loss of the payload despite rocket recovery, payload recoverability and sturdiness have been placed under increased scrutiny. We thus switched to a non-deployable design, with a multi-stage, steel and aluminum "wedding cake" structure housed in the nosecone, shown in figure 42 above. Similar to the one used on our 30k COTS rocket at SAC 2018, the improved design reduces the weight by 60% while maintaining structural integrity under 2800 lbs, twice the worst expected load. This integrity was verified through FEA analysis, the results of which are shown in figure 43. Note that the rods and plates are made of 6061 T6 aluminum (200 MPa yield strength), while the topmost plate is made of 1045 cold rolled steel, a high strength alloy (530 MPa yield strength). The reduced structural weight also frees up weight for the scientific experiment and associated equipment. Similarly 3D printed components were upgraded from PLA to PETG for its higher strength and glass transition temperature.

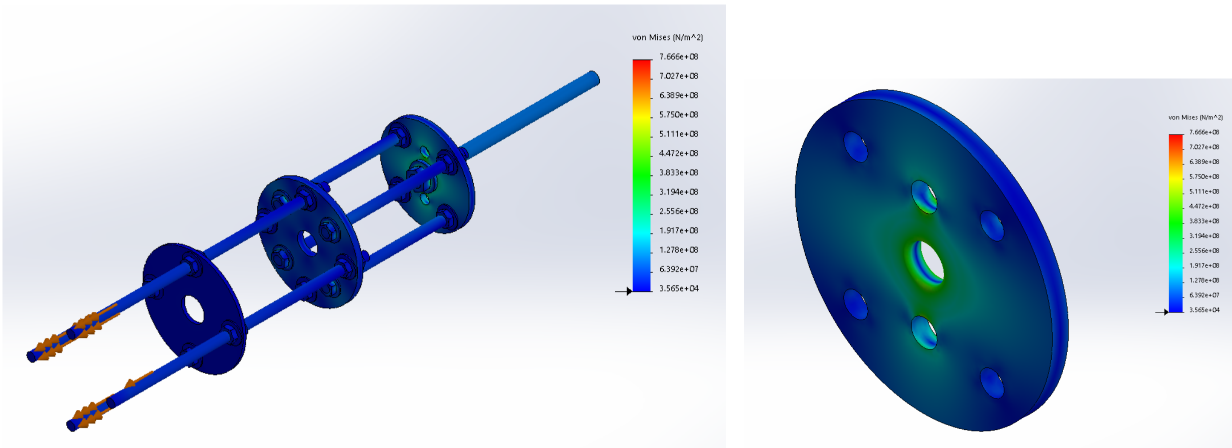

(a) Overall view of FEA results.

(b) Top plate under highest stress.

Fig. 43 Payload structure under 2800lbs of load, double the worst-case loading.

Microorganism collection has also been increased in terms of quantity and quality. The general collection principle consists of filtering the ambient air through gamma-sterilised gelatin filters by 12V diaphragm vacuum pumps. These filters were chosen as they can easily be dissolved into an agar bed or a solvent for bacterial growth and PCR analysis. Gamma sterilisation ensures they are free from any DNA contaminants, which is relevant for PCR.

Previous collection was performed on two gelatin filters contained in a sterilized open-air button sampler, drawing at an estimated rate of 4 lpm from ten to one thousand feet, leading to concerns regarding sampling volume and contamination. To alleviate contamination concerns, the filters are held in sealed filter cassettes, connected on one side to the pumps and on the other to the inlet. The system will be sealed upstream by a a normally closed electric pinch valve, whose configuration limits pressure drop and reduces contamination. The downstream seal is ensured by the pumps, which act as back-flow prevention valves. Therefore air sampling occurs only during the intended window. The effects of any prior contamination are mitigated by sterilisation of the pneumatic circuit. Moreover, as the air inlet opens during the ejection, a plug seals the inlet to prevent black powder from entering the tubing. This plug is connected to the free plate, and thus will be pulled out of the inlet upon separation.

In total, 5 filters will be tested. During descent, 3 filters will perform the actual sampling, whereas a fourth will be kept alongside in a sealed cassette to estimate a contamination baseline, and a fifth will be used for a ground-level sample as a reference.

Sampling volume was increased by adding a second vacuum pump, improving the flow to 15 lpm measured at the system inlet. This is to be compared to the theoretical airflow of 24 lpm. In addition, as sampling starts at 29,500 ft, total collection time has also been increased.

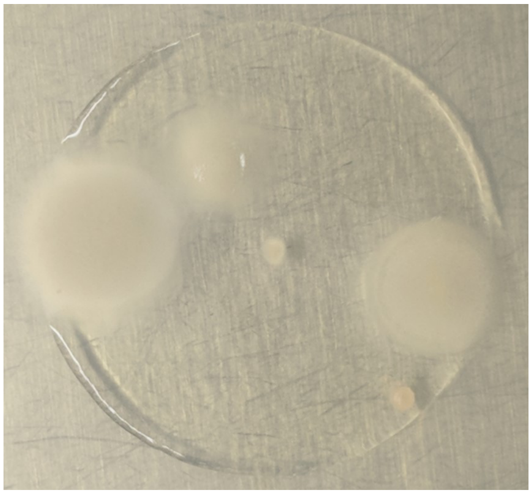

(a) Bacteria Colonies grown on agar plates

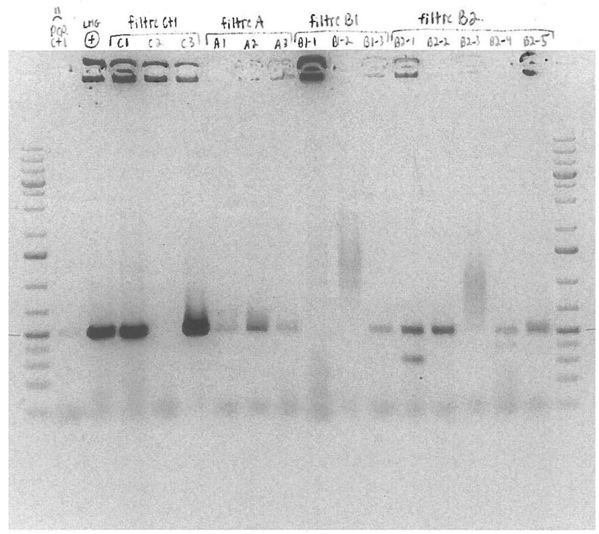

(b) PCR Assays done by MI4

Fig. 44 Lab Results from Testing in April 2019

AMOSE is controlled by a Teensy 3.5 micro-controller which will be used in combination with a sensor suite to determine when to activate and deactivate the pumps run the experiment, and provide contextual data. The sensors include an MPU9250 IMU for measurement of acceleration, temperature, and spin; a DHT22 humidity sensor measuring temperature and humidity; and a barometer to measure atmospheric pressure and calculate the height of the payload.

Upon reaching apogee, the nosecone will separate from the rocket and the plug in the air inlet, attached to the shock cord, will be pulled out by the force of the ejection charges, allowing airflow into the system. Shortly after this around 29500 ft, the electronics will send a signal to the valve to open it, as well as to the vacuum pumps to activate them. The system will run until directly before the main parachute opens at roughly 1,800 ft, at which point the pumps shut off and the pinch valve closes, sealing the system from airflow after an estimated sampling time of 4min 30 s

Upon recovery, the cassettes will be removed from the nosecone and clamped shut on either side to prevent contamination during transport. They will be placed within sterilized bags, which will be placed within an insulated box to prevent temperature fluctuations. This box will be sealed until it can be returned to McGill University for analysis by The MI4 lab. Each filter will dissolved, with one half used for plating and the other for PCR.

III. Mission Concept of Operations Overview

Caladan has a typical sounding rocket mission, with a non-deploying payload that will need to activate and deactivate at specific altitudes. This adds additional mission phases but otherwise will not affect the overall expected trajectory.

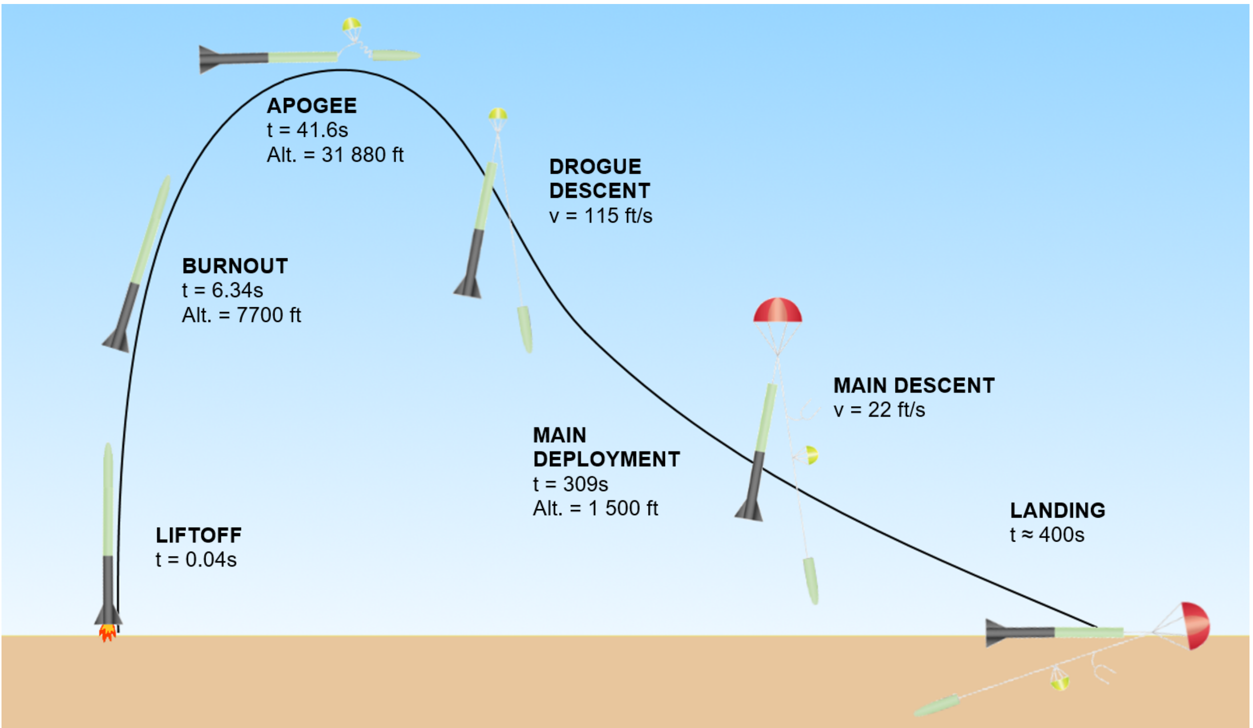

Fig. 45 Mission phases of Caladan.

Phase	Description
1. Pre-arming Launchpad Installation	The rocket is manually slid onto the launch rail, secured using 1515 rail buttons. Telemetry is active and transmitting to a ground station. The launch rail angle is adjusted based on the results of simulations performed using the day's weather conditions.
	Energetic circuits are activated using a combination of switches and push buttons.
2. Arming	Energetics circuitry is brought online, and an audio cue will confirm continuity. Igniters are installed, connected to the competition power supply and checked for continuity. Rocket should remain inert. Personnel are evacuated following successful continuity checks.
	The launch button is pressed following authorization by competition officials.
3. Ignition t = 0.00s	A current is sent through the igniter. The fuel grains light and a smoke plume becomes visible. Telemetry continues to be received
	First vertical motion of the rocket.
4. Lift-off t = 0.04s	The rocket accelerates upward and clears the launch rail at 119 ft/s and a stability margin of 1.75.

The rocket clears the launch rail.

5. Powered Ascent t = 0.32s	The rocket motor continues to burn and accelerate the rocket. Max-Q, or maximum dynamic pressure, is reached at t = 4.75s, slightly before motor burnout.

Motor burnout at the specified time.

6. Unpowered Ascent t = 6.34s	A smoke charge continues to burn to improve visibility of the rocket. The rocket coasts upward until the apogee at 31,880 ft AGL.

Pressure sensors detect apogee and an electrical signal is sent to the ejection charges, detonating them.

7. Drogue Deployment and Controlled Descent t = 42.6s	Ejection charge detonation pressurizes the small ejection compartment, breaking the shear pins and popping off the nose cone. The drogue chute is pulled out and immediately unfolds, slowing the rocket's descent to approximately 100 ft/s. The descent speed decreases with altitude as the air density (and subsequently drag) increase.

The payload pinch valve opens and the pumps begin running.

8. Payload Activation t = 47.5s	Shortly after apogee and drogue deployment, air begins flowing through the payload plumbing and the payload begins collecting samples. This occurs at a preset altitude of 29,000 ft.

The payload pinch valve closes and the pumps turn off.

9. Payload Deactivation t = 305s	Shortly before main deployment the payload will deactivate and seal itself. This will occur at a preset altitude of 1,800 ft.

Electrical signal is sent to tender descenders, igniting the explosive charge.

10. Main Deployment t = 309s	At 1,500 ft AGL, the tender descenders separate and the drag forces on the drogue chute pull out the main chute. The main fully unfolds and slows the rocket to 20.9 ft/s, a safe value for ground impact. Telemetry should still be active.

The rocket hits the ground and a recovery team is dispatched with a GPS tracking device.

11. Ground Recovery	The rocket is retrieved by the recovery team. The payload is extracted and sealed on-site to prevent ground contamination. Upon return to base camp, the payload is double-bagged and stored in a cooler until it can be sent to a lab for analysis.

IV. Conclusions and Lessons Learned

A. Technical Lessons Learned

With an ever-increasing emphasis on testing, the team has begun to realize the importance of proper test documentation, particularly in avionics where the test results are very sensitive to the experimental setup. We anticipate that proper documentation will become increasingly important as the team transitions to the development of SRAD motors.

As the team's designs become more complex, the team has found that certain elements succumbed to 'analysis paralysis', leading to time crunches. To combat this, the team will attempt to instill a 'rapid prototyping' mentality, where designs are tested and iterated upon as quickly as is feasible, even at the expense of higher costs due to more discarded and flawed designs. This is in line with the the team's overall philosophy of iterative improvement and physical testing, as the team's software analysis capabilities are not sufficiently sophisticated to ensure good designs on the first attempt.

Additionally, to keep up with more complex projects and ever-changing requirements between different subteams, the team made its first foray into implementing systems engineering practices, although the results will not be visible during this years' design cycle.

With regards to safety, the team has witnessed lax safety practices adversely affect the relationship between university faculty and other design teams, and as such the team has taken great pains to proactively improve safety practices, including voluntarily submitting the workshop to Environmental, Health & Safety inspections, compiling an inventory of chemicals, creating incident report forms, instating mandatory WHMIS training as well as MSDS quizzes. This is especially important as the team grows larger, with unprecedented levels of membership and retention this year, making it more difficult to properly hold people accountable for safety without a good system.

B. Non-Technical Lessons Learned

As the team grows, the team has found that it is important to ensure that every member is made to feel like a useful contributing part of the team, performing meaningful work, but this means that less experienced members need to be heavily involved with projects from the beginning. The high level of technicality and knowledge base of some of the experienced leads can be very intimidating for new members, and in the same vein it can be difficult to view the team from the perspective of a new member as a seasoned lead. To "bridge the gap" better, the team will be organizing more team-bonding activities and social events, based off of member feedback.

As the team matures, knowledge transfer has become one of the primary non-technical concerns, to be outlined in detail in the following section. In the past, an informal and flat leadership structure was used, with roles being very loosely defined. However, with the continued growth of the team, now and for the foreseeable future, a more formal management structure was needed, as team leads often now have more administrative tasks than technical tasks due to the sheer size of their subteams. To that end, a role flowchart and definition list was codified.

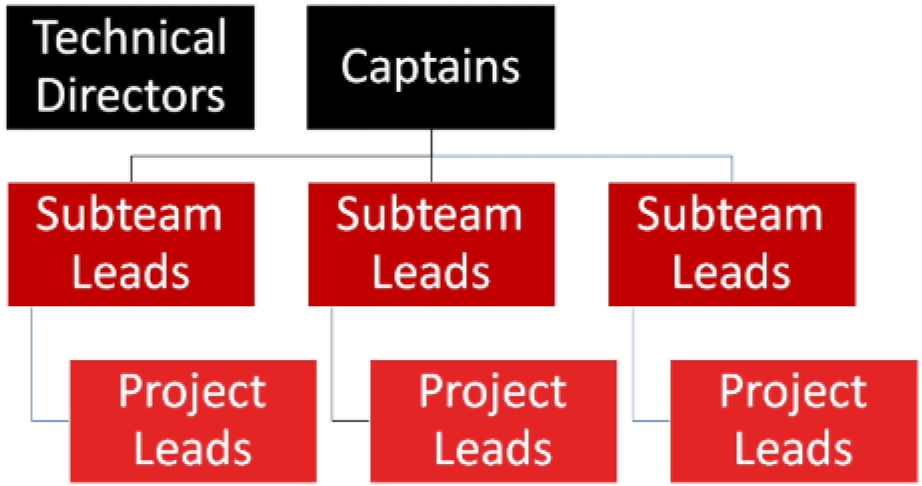

Fig. 46 MRT management structure

C. Knowledge Transfer

This is the fifth year since MRT's creation and is the first year that the team has had to deal with significant member turnover and knowledge transfer challenges, due to the first generation of experienced team members graduating. As there is another wave of key members graduating this year, there was a significant effort to decrease the degree to which the team relies on single individuals. One of the main initiatives was the creation of an MRT 'bible', containing tips and guidelines on how to properly administer the team as well as hard-to-find technical information.

Additionally, subteam-specific reading lists are being made to help fresh members direct their efforts toward learning the most useful information. The MRT has created a large body of technical and educational resources on its team-wide cloud storage. Of course, merely giving members a large body of information to read is not sufficient for proper knowledge transfer, and therefore an effort is being made to ensure leads are more accessible to newer members. To this end, the 'lead' meetings were made open to all members to attend, and key graduating members are asked to remain accessible through team communication channels. More broadly speaking, the team will be focusing on three main methods of knowledge transfer:

1) Storytelling: the complimenting of reports and formal documentation with the stories that surround them.
2) Process mapping: process used to identify users of knowledge as well as knowledge dispersion, by illustrating the internal processes of an organization (identifying decision makers, decision rationales, etc.). In practice, this process map outlines the structure of operation within the team.
3) After action reviews: documentation of lessons learned either throughout a project or after its completion. In practice, these start out as a set of notes from project team members and end up as a summary of the lessons learned, with the specifics contained in the notes.

Knowledge transfer is not limited to general members; it must also be done between junior leads and senior leads. To this end the team has introduced transition meetings to ensure future technical leads will be aware of their expectations as well as how to properly perform their roles.

D. Conclusions

Overall, this year was a year of growth and transition for the team. Emphasis has been increasingly placed on training and testing infrastructure. While many of the team's projects are not ready to be demonstrated this year, the team is positioning itself to succeed and work on innovative projects in future years.
Caladan is a continuation of the MRT's design philosophy of incremental improvement while making mistakes and learning from them. As such, Caladan's design was intended to make small adjustments to proven subsystems while

making major improvements to subsystems that historically had poor performances. Just like how the planet Caladan was a safe haven for House Atreides, *Caladan* is the final step, before getting into riskier, but ultimately more thrilling waters.

Appendix 1: Systems Weights, Measures and Performance Data

Spaceport America Cup

Intercollegiate Rocket Engineering Competition
Entry Form & Progress Update

Color Key

SRAD = Student Researched and Designed

v19.1

IMPOTANT CHANGE EFFECTIVE IMMEDIATELY FOR SA CUP 2019 EVENT
All inputs are mandatory for all submitions of this document. We undestand some data may change over time, this is completely acceptable.

Feel free to add additional commanets where needed, and be sure to fill out the last page. Treat the last page as a "cover letter" for your project.

Date Submitted: 111618 [1]

Team ID: 21

* You will receive your Team ID after you submit your 1st project entry form.

Country: Canada

State or Province: QC [2]

State or Province is for US and Canada

Team Information

Rocket/Project Name:	Caladan [3]
Student Organization Name	McGill Rocket Team [4]
College or University Name:	McGill University [5]
Preferred Informal Name:	Optional [6]
Organization Type:	Club/Group
Project Start Date	1/9/2018 [7]
Category:	30k – COTS – All Propulsion Types

Projects are not limited on how many years they take

Member	Name	Email	Phone
Student Lead	Liem Dam-Quang	liem.dam-quang@mail.mcgill.ca [8]	5144311559
Alt. Student Lead	Daniil Lisus	daniil.lisus@mail.mcgill.ca [9]	4389298328
Faculty Advisor	James Forbes	james.richard.forbes@mcgill.ca [10]	5143987142
Alt. Faculty Adviser	Stephen Yue	stephen.yue@mcgill.ca [11]	5143981378

For Mailing Awards:

Payable To:	McGill EUS - attn: McGill Rocket Team
Address Line 1:	McConnell Engineering Building, Rm 7
Address Line 2:	3480 University St.
Address Line 3:	Montreal, QC
Address Line 4:	H3A 0E9
Address Line 5:	

Demographic Data

This is all members working with your project including those not attending the event. This will help ESRA and Spaceport America promote the event and get more sponsorships and grants to help the teams and improve the event.

Number of team members

High School	0	Male	110
Undergrad	158	Female	50
Masters	2	Veterans	0
PhD	0	NAR or Tripoli	0

Just a reminder the you are not required to have a NAR, Tripoli member on your team. If your country has an equivelant organization to NAR or Tripoli, you can cant them in the NAR or Tripoli box. CAR from Canada is an example.

STEM Outreach Events

students and professionals alike. For example, a few members gave a presentation about rocketry and science at Académie Yechiva Yavne, a local elementary school. The team also tabled with hands-on activities at Montreal's Planetarium for the International Astronomy day, along with other Montreal aerospace groups. On the professional side, the team tabled at the Quebec Order of Engineers' colloquium, and the McGill Institute of Aerospace Engineering annual luncheon. The Team joined and promoted the “Don’t Let Go” movement spurred by MDA in the hopes of expanding the aerospace industry within Canada, which led to a new Canadian Space Strategy. It is also registered for the trial run of the “Launch Canada” competition in late August 2019, with an inauguration in 2020. We are also in contact with CEGEPs to organize "design sprints" where students build small SRAD low power rockets, simulate their flight using OpenRocket, and then fly them. We are in talks to collaborate with Dawson college on a payload project for their independent study program. We hope our efforts provide the opportunity for young individuals to explore their interest in rocketry and promote exposure to

Rocket Information

Overall rocket parameters:

	Measurement	Additional Comments (Optional)
Airframe Length (inches):	126 [12]	
Airframe Diameter (inches):	5.2 [13]	
Fin-span (inches):	11 [14]	
Vehicle weight (pounds):	41.61 [15]	
Propellent weight (pounds):	24.06 [16]	
Payload weight (pounds):	8.8 [17]	
Liftoff weight (pounds):	74.47 [18]	
Number of stages:	1 [19]	
Strap-on Booster Cluster:	No [20]	
Propulsion Type:	Solid [21]	
Propulsion Manufacturer:	Commercial [22]	
Kinetic Energy Dart:	No [23]	

Propulsion Systems: (Stage: Manufacturer, Motor, Letter Class, Total Impulse)

1st Stage: Cesaroni Pro 98, 21062O3400-P, O Class, 21062.2 Ns
[24]

Total Impulse of all Motors:	21062.2 [25]	(Ns)

Predicted Flight Data and Analysis

The following stats should be calculated using rocket trajectory software or by hand.

Pro Tip: Reference the Barrowman Equations, know what they are, and know how to use them.

	Measurement	Additional Comments (Optional)
Launch Rail:	ESRA Provide Rail [26]	
Rail Length (feet):	17 [27]	
Liftoff Thrust-Weight Ratio:	13.54	
Launch Rail Departure Velocity (feet/second):	119	
Minimum Static Margin During Boost:	1.67	*Between rail departure and burnout With windspeed of 7.2mph
Maximum Acceleration (G):	14.65	
Maximum Velocity (feet/second):	1919	
Target Apogee (feet AGL):	30K [28]	
Predicted Apogee (feet AGL):	31880	Simulation software (OpenRocket) tends to have optimistic predictions, and the current overshoot also gives a margin for slight changes that arise during manufacturing

Payload Information

Payload Description:

The payload will be a functional biological experiment. Its main purpose is to collect atmospheric micro-organisms for on-ground analysis and characterization, in order to identify bacterial strains in the mid to high-altitude troposphere. The experiment will be housed in a non-deployable internal structure housed in the nosecone and mainly consist of an automated air filtration system. The payload components will include a pneumatic circuit for sampling, filters, which will capture the bioaerosol on its surface, and a cassette-type housing which encases the filters. The electronics system will be composed of a Teensy microcontroller coupled with a weather sensor suite (which measures pressure, temperature, and hygrometry), controlling the valve and pump activation.

measures pressure, temperature, and hygrometry), controlling the valve and pump activation.

In order to avoid contamination by ground-level microorganisms, multiple measures will be taken. Firstly, the pneumatic circuit will be kept shut before and after sampling by a valve controlled via the Teensy system. This valve, normally closed, will only open at the desired altitude and will shut before the main parachute is deployed. The pumps contain backflow preventions, and thus no backflow can contaminate the filters. Additionally, each element of the pneumatic tubing, with special attention to elements in contact with the airflow upstream from the filters, will be sterilized with ethanol in a sterile biological cabinet, located in a controlled laboratory environment.

The sampling of micro-organisms will occur during the descent, between the separation of the rocket and 1,500ft above ground. A plug for the inlet, attached to the drogue's shock cord, will conserve the integrity of the system and its sterilization, until the rocket is separated, which will thus pull the plug off. A time delay after the separation of the rocket is in place, such that the valve is opened slightly after the rocket is separated. This is to ensure that no black powder residue will enter the tubing. The main triggers to open the valves and start the pumps is a pressure based altitude sensor, with a secondary redundancy of an accelerometer/gyroscope.

The experiment design also includes blank filters onboard the rocket, which will not be subject to the pressurized flow of air to measure background exposure and possible contamination. Ground level sampling will also be performed for comparison. Once the rocket has been recovered, the samples will be removed from the nosecone, clamped such that the system will still be closed. The cassette enclosures will be placed in an insulated box from New Mexico to Montreal. This will allow the samples to experience a nearly constant temperature until we arrive at the laboratory, which ensures maximum viability of the data collected. The samples will then be analyzed with the collaboration of the McGill Interdisciplinary Initiative on Infection and Immunity (MI4). The analysis will be done by culture growth on agar gel and microscopy, as well as genome sequencing. Results from this analysis will will focus on the identification of the micro-organisms collected at high altitudes during the flight of Caladan.

Recovery Information

The recovery sequence consists of a single separation, double deployment system.

The separation event happens at the base of the nose cone at apogee. The separation results from a black powder pyrotechnic charge that causes the pressure in the ejection chamber to build up and break the shear pins holding the nose cone to the rest of the rocket. The volume of the ejection chamber is designed as small as possible to minimize the amount of black powder needed. Two charge wells are present and each is connected to an independent ejection circuit for redundancy. Both charge wells are airtight to ensure that enough oxygen is available at apogee for complete combustion of the black powder.

Once separation is completed, the drogue parachute is pulled out of the rocket by the nose cone moving away from the rocket. The rocket and the nose cone then descend under drogue for most of the descent. The tender descenders (pyrotechnic links) ensure that the main parachute remains in the rocket.

At an altitude of 1000ft, the tender decenders detonate and the main parachute is pulled out of the rocket by the drogue parachute. Two tender desenders in series are connected to two independent ejection circuits for redundancy.

All components of the rocket are recovered together, as the nose cone and the rest of the rocket body remain connected for the entire recovery sequence.

The black powder ejection system, tender descenders, shock cords and parachutes are all SRAD.

Both separation events are controlled by two independent ejection circuits, one SRAD and one COTS. For each event, the SRAD ejection circuit uses two relays in series that are each controlled by an individual pin on the microcontroller. In order for a current to be sent along the e-match, which is connected to the second relay in the series, both pins on the microcontroller must send a high signal to their respective relays. This redundancy is to ensure that no fluctuating voltages from the microcontroller accidentally triggers a relay and inadvertently ignites one of the ematches.

There will be triple redundancy telemetry systems, which include a COTS flight computer, an SRAD telemetry system, and a GPS redundancy system exclusively for transmitting GPS data as a backup.

Planned Tests

* Please keep brief

Date	Type	Description	Status	Comments
11/16/18	Ground	RF tests in anechoic chamber with 2 dBi antennas, using preliminary system design	Minor Issues	Was able to measure the attenuation of the fiberglass body tube but only tested for vertical 0°, horizontal 0°, and horizontal 180°. Missing data to plot the full radiation pattern.
11/24/18	Ground	Black powder ejection system tests, using preliminary system design	Minor Issues	Potential improvements to system identified
1/15/19	Ground	RF range tests with 2 dBi antennas, using preliminary system design	Minor Issues	Was able to receive data packets from up to 2.6km range under unfavorable weather conditions. Did not test throughput and attenuation of fiberglass in outdoor conditions.

1/18/19	Ground	GPS module outdoor testing inside the airframe with and without extension LNA antenna	Successful	Was able to gather Signal-to-Noise Ratio data from the GPS connection to the satellites with and without the extension LNA antenna
1/20/19	Ground	Black powder charge well containment tests	Successful	Different charge well configurations tested
2/9/19	Ground	Overall black powder ejection system tests using improved system design	Successful	Entire system was tested multiple times with different amounts of black powder and different chamber structural configurations
2/15/19	Ground	Power Management PCB testing	Successful	Prototype was manufactured, but PCB layout needed to be revised. Testing will occur when the revised PCB is manufactured.
2/28/19	Ground	RF tests in anechoic chamber with 2 dBi antennas, using improved system design	Successful	The most important and essential anechoic chamber tests with the new xtend vb modules have been completed.
2/28/19	Ground	Ejection PCB testing		PCB has been fabricated, waiting for components to be soldered so board can be tested.
2/28/19	Ground	Ground station software testing	Minor Issues	Preliminary version of the ground-station code is complete, but there are a few bugs that need to be fixed and additional features we want to implement.
2/24/19	Ground	Testing of payload components (individually)	Successful	Measuring airflow of pumps and voltages of batteries
3/10/19	Ground	Payload Full System Integration and Test	Minor Issues	Tubing, pump, and cassette system was successful. Minor issues in connection between cassette and tubing occured
3/15/19	Other	Compressive load testing on body tube	TBD	To validate CF layup, since different from previous year
3/15/19	Ground	RF range tests with 2 dBi antennas, using improved system design	Successful	Will be occuring this weekend using a COTS 1.5dBi patch antenna with an 11.5dBi receiver yagi antenna.
3/15/19	Ground	SRAD antenna tests in anechoic chamber, using SRAD antenna design	TBD	SRAD antennas cancelled due to time constraints
3/15/19	Ground	Telemetry PCB testing	Successful	First iteration of PCB has been completed, but design issues were found upon fabrication that will be fixed for the second iteration of the boards.
3/15/19	Ground	GPS Redundancy PCB testing	Successful	PCB layouts were completed, but also ran into the same design issues as the telemetry board, which must be fixed for the second iteration of the boards.
3/23/19	Ground	Ejection charge well containment test in vacuum	TBD	Unable to source proper size vacuum chamber in time.
3/29/19	Ground	SRAD antenna range tests, using SRAD antenna design	TBD	SRAD antennas cancelled due to time constraints
3/31/19	Ground	Payload Full System Integration and Test #2	Successful	Second full-system test was done after steilizating components with the assistance of MI4. After 5 min of optimal airflow in an open environment (outside), filters were taken back to the lab and prepared for culture growth. Various cultures were successfully grown from this test.
3/31/19	Ground	Circuits vibration tests, using improved system design	TBD	
4/20/19	Ground	Full Systems Test	TBD	Full system assembly and ground testing
5/7/19	Ground	Long range ground station telemetry test	Successful	Ground station succesfully parsed 97% of all recieved telemetry data at a distance of 10km
5/18/19	In-Flight	Full avionics systems flight test	TBD	Launching a test rocket to test avionics setup
5/18/19	In-Flight	In-flight recovery test	TBD	Launching a test rocket to test recovery setup
5/18/19	In-Flight	In-flight payload test	TBD	Launching a test rocket to test payload setup

Any other pertinent information:

Caladan is McGill's third attempt at the 30k COTS category. Having failed to recover the previous two attempts, we hope to make our third attempt successful. This project follows MRT's philosophy of incremental improvement, and rigorous testing. In broad strokes, this rocket is very similar to last year's in many respects: It uses the same commercial motor, has the same outer diameter, and uses the same recovery scheme. (Our previous years' 30k project was itself largely similar to McGill's winning 10k COTS rocket, Blanche.)

The internal structures have been extensively redesigned based off of lessons learned from last year. Historically, avionics have been a weak point in our designs and were the primary reason we failed to locate our rocket last year, after losing telemetry shortly after takeoff. For that reason, our avionics have been redesigned from the ground up, featuring more redundancies and more SRAD components than last year. We are designing a complete ground station setup. To aid this redesign, we are introducing many more tests to ensure the robustness of our electronics.

In terms of our internal structure, we have found that we are able to significantly simplify it thanks, in part, to our advanced SRAD composites. Despite having more features than our previous 30K rocket, Caladan will be half a foot shorter and 5 lbs lighter, allowing for more leeway to hit our target apogee.

The recovery scheme is single-separation, dual deployment - the same as last year - but has had its wiring revised, increasing simplicity, compactness and ease of packing.

Caladan is the culmination of all the lessons we have learned after 4 years of launching COTS rockets and is representative of the iterative approach that has served the McGill Rocket Team so well. Caladan is a demonstration of the importance of having solid fundamentals.

End of File

Appendix 2: Project Test Reports

Recovery System Testing

Table 5 Outline of Tests 2018-2019

Subsystem	Description	Result
Recovery	Tender-Descender functionality test. Attach weights to device until separation is achieved.	35lbs required for separation.
Recovery	Tender-Descender functionality test. Simply close device and force separation with black powder charge.	Success
Recovery	Ground test of structural integrity of plate and coupler ring stopper setup. Force separation using 2.0 grams of black powder for a 137 cu. in. chamber and a safety factor of 1.3. Test is successful if the nose cone separates.	Success
Recovery	Series of tests for shear pin strength. To determine the actual strength of nylon screws vs theoretical values. Force separation using 1.4 grams of black powder for a 137 cu. in. chamber and a safety factor of 0.98. There should be about 50% chance of the nose cone separating.	Success - The nose cone separated 1 time out of 3.
Recovery	Prototype charge well containment test 1. Place sealed charge well with silicone cap inside a vacuum chamber and pull vacuum. Test is successful if the silicone cap remains sealed.	Success
Recovery	Prototype charge well containment test 2. Detonate a black powder charge inside a prototype charge well in a vacuum chamber to determine the percentage of black powder particles that have undergone combustion.	Pending Facility - Currently trying to get access to a large enough vacuum chamber.
Recovery	Full chamber ground test using an improved design. Pack ejection chamber with shock cords, charge wells, and payload plug. Detonate 0.42 grams of black powder in a 30 cu. in. chamber with a safety factor of 1.29. Test is successful if the nose cone ejects, pulls the free plate out of the tube, and pulls out the payload plug.	Success
Recovery	Classic semi-elliptical parachute test. Check for inflation and examine descent rate though video analysis from previous launches. To obtain a more accurate drag coefficient.	Success - Drag coefficient of approximately 1.65.
Recovery	Pull-down apex parachute test. Drop test, check for inflation and examine descent rate with altimeter. To obtain a more accurate drag coefficient for the new parachute design.	Pending Launch - May 18th 2018
Recovery	Full in-flight deployment sequence test. Verify nose cone ejection, successful drogue deployment, successful main parachute retention, successful main parachute deployment w/ tender descenders.	Pending Launch - May 18th 2018

SRAD Propulsion Systems Testing

THIS PAGE INTENTIONALLY LEFT BLANK

SRAD Pressure Vessel Testing

THIS PAGE INTENTIONALLY LEFT BLANK

Avionics System Testing

Table 6 Outline of Tests 2018-2019 **Subsystem**

Description	**Result**	
Avionics	Test basic transmission between XBee Pro S3B transceiver RF modules. Sent basic string to simulate telemetry data being sent during launch	Success
Avionics	Measure the signal strength, data throughput and packet error rate of the XBee Pro S3B radios.	Success
Avionics	Observe the difference between expected and experimental RSSI when adding attenuation to radio transmission between two XBee Pro S3B radios.	There is a largest difference between expected and experimental RSSI at higher attenuation.
Avionics	Anechoic chamber test to observe the effects on RSSI using XTend RF modules with and without the fiberglass body tube as well as different orientations of the transmitter.	Success
Avionics	Long range test at 15 Km to observe the characteristics of out XTend RF modules and understand the radio's limits.	Success
Avionics	Test the effects of two transmitting XTend RF modules in close proximity to observe the effects on the data sent.	We observed a noticeable difference when both RF modules were transmitting, in packets with error and in RSSI.
Avionics	Test the different hopping sequences during radio transmission of the XTend RF modules to understand the best setting to minimize interference between two radios.	Success - We concluded that the hopping parameter 6 and 9 result in the lowest amount of interference between the two radios.
Avionics	Long range test at 10 Km with finalized telemetry code and antenna setup to simulate launch.	Success
Avionics	Observe the difference in data rate and RSSI when transmitting constant sized data strings or a combination of small and larger data strings.	Observed that constant sized data string results to best performance.
Avionics	GPS testing to select the Adafruit LNA external active ceramic patch antenna as the most performing one. Measure the effect of different surrounding material.	Success.
Avionics	Observed intermodulation when powering both radios at the same time using a spectrum analyzer to test the harmful interference between the two transmitters	Success - Observed noticeable intermodulation between two XTend RF modules.
Avionics	Spin test	Success - Maintained stable telemetry link.
Avionics	Antenna radiation pattern test	Success - Selected the Taoglas FXP.400 to be mounted upside down, facing inwards on the inner side of a fiberglass coupler.

Avionics	Ejection Apogee detect test	Success - System correctly determines the apogee event based on barometric variations and subsequently activates the drogue and main parachute deployment charges
Avionics	Power Management output voltage quality	Success - Ripple measured to be less than 5mV peak to peak at maximum design load and operating load

Appendix 3: Hazard Analysis

Hazardous Material	Storage	Handling	Transportation	Risk of Mishap and Rationale	Mitigation (Process/Design)	Risk of Injury after Mitigation
Black Powder	`	When used for testing avoid impact, friction, heat, sparks and open flame. Use instruments to measure and load, don't touch directly. Limit the number of personel in vicinity.	Kept in a box surrounded by padding to prevent vibration or jolts while driving.	Low	Restricted acess to select individuals on the team with experience and care. Recieved at competiion on site. Prepare Black Powder energetics only immediately prior to full assembly.	Very Low
Fuel Grains	Ensure it is kept cool away from direct sunlight, heat, sparks, friction, and impact.	Gently carry and install into vehicle, with care not to cause any impact. Limit the number of personel in vicinity.	Secured in a Nanuk foam lined container during transportation to prevent unwanted impacts or vibrations.	Low	Restricted access to select individuals on the team with experience and care. Recieved at competition on site.	Very Low
LiPo Batteries	Cool, dry areas, inside of a LiPo bag	Avoid heat and flammable substances. Leave no exposed leads to batteries.	Store in LiPo bags for transportation. Do not leave in car without AC running to prevent excess heat. Do not allow direct sunlight on bag or batteries.	Low	Careful manipulation, taking caution to not create a short-circuit. Proper storage and avoiding sources of heat at all times, especially in desert.	Very Low
E-Matches	Stored in a dry lockable cabinet away from black powder, or any other flammable substances. Kept grounded to avoid accidental trigger	Careful when handling to ensure circuitry doesn't prematurely detonate.	Transported in a separate container from other potential flammables or combustibles. Kept grounded at all times.	Low	Restricted acess to select individuals on the team with experience and care. Recieved at competiion on site. Do not connect E-Matches to power source until right before completing full assembly.	Very Low
Epoxy	Stored in dry cabinet, at room temperature	User should wear gloves at all times and respirators in the case that the work space is not properly ventillated.	Transported in dry container. Taken out of car when AC is not turned on to maintain temperature range	Low		Very Low

Appendix 4: Risk Assessment

Team	Rocket Name	Date
21	Caladan	May 17, 2019

Hazard	Possible Causes	Risk of Mishap and Rationale	Mitigation Approach	Risk of Injury after Mitigation	Overseeing Division	Mission Phase
Explosion of solid rocket motor, leading to personell injury	Cracks in propellant grain	Low	Pressure test motor case (with end closures) to 1.5 maximum expected operating pressure	Low	Propulsion	Phase 4 - Lift off Phase 5 - Powered ascent
	Debonding of propellant from wall	Low	Visually inspect motor grain for cracks, debonds, and gaps during and after assembly	Low	Propulsion	
	Gaps between propellant sections and/or nozzle	Low	Use ductile (non-fragmenting) material for motor case	Low	Propulsion	
	Chunk of propellant breaking off and plugging nozzle	Low	Inspect motor case for damage during final assembly before launch	Low	Propulsion	
	Motor case unable to contain normal operating pressure	Low	Minimal crew number at assembly pad, located 200 feet from rocket at launch/flight	Low	Propulsion	
	Motor end closures fail to hold	Low	Launch crew 200 feet from rocket at launch, behind barrier (vehicle)	Low	Propulsion	
Rocket deviates from nominal flight path, comes in contact with personnel at high speed	One or more fins broke off	Low; physical testing of fins validate high safety factor	Simulate fins at critical points in flight, use U-G method to calculate flutter and divergence velocities	Low	Aerodynamics	Phase 5 - Powered Ascent
	Rocket becomes aerodynamically unstable	Low; proper analysis done	Proper simulation and analysis to guarantee stability. Physical measurement of CG to validate simulation. Precision manufacturing to further validate assumptions made in simulation.			
	Body tube shatters.	Low; body tube is tested for maximum load.	Test carbon fibre samples, apply loads to test sections of body tube, complete FEA			
Recovery system fails to deploy, rocket comes in contact with personnel	On-board electronic separation/altitude aquisition systems fail	Low; several built in redundancies.	Testing of primary systems for reliability, in addition to redundant strataloggers and independant battery sources.	Low	Avionics	Phase 7 - Drogue deployment and controlled descent Phase 10 - Main deployment
	Pyrotechnic separation fails.	Low; tested for reliability.	Excess black powder for high safety factor of over 2, ensures separation even if 50% of blackpowder is not ignited.	Low		
Recovery system partially deploys, rocket comes in contact with personnel	Parachutes get tangled.	Medium; orientation can be unpredictable in flight.	Professionally packed parachutes to ensure proper deployment. Clear exit paths for parachute to open fully. Multiple ground ejection tests. Test rocket flight test.	Low	Structure	Phase 7 - Drogue deployment and controlled descent Phase 10 - Main deployment
Recovery system ejection occurs before expected flight phase	Unforseen software bugs or noise in sensors cause a premature detonation.	Medium; nature of coding is prone to mistakes	All circuits directly collected to energetics are "safed" (i.e. circuit is open) until rocket is ready for motor ignition.	Low	Avionics	Phase 1 - Installation; Phase 2 - Arming
	Ejection circuit short-circuits, triggers without controller input	Low	Extensive wiring and circuit testing is done. Ejection circuit wires are fully insulated and not in near contact to any hot wires.	Low	Avionics	
Main parachute deploys at or near apogee, rocket or payload drifts to highway(s) or on base camp	Incorrect wiring or software bugs	Medium; nature of coding/wiring is prone to mistakes	Repeated software testing, proper cable management, labeling, and repeated checks for wiring.	Low	Avionics	Phase 6 - Unpowered ascent Phase 7 - Drogue deployment and controlled descent

Rocket does not ignite when command is given ("hang fire"), but does ignite when team approaches to troubleshoot	Delayed burn due to improper ignitor set up.	Low; ignitors are very effective	Properly set up ignitor. If 'hang fire' occurs, wait prolonged period (5-10 min) before approaching rocket.	Low	Propulsion	Phase 3 - Ignition
Rocket falls from launch rail during prelaunch preparations, causing injury	Launch lugs broke off	Low; launch lugs will be sufficiently tightened	Use loctite for additional safety	Low	Aerodynamics	Phase 1 - Installation
Premature ignition	Sparks, embers (smoking), improper grounding for igniter	Low; engine will be handled with care	Prevent propellant valves from opening, ensure ignitor is properly grounded prior to arming	Low	Propulsion	Phase 1 - Installation; Phase 2 - Arming
Power Loss	Batteries not fully charged. Severed wires due to high acceleration.	Low	Batteries of the same voltage placed in parallel and charged the night before launch. Batteries tested with multimeter before flight. Connections soldered on rather than plugged in. Power management circuit adds redundancy in the event of a lost battery	Low	Avionics	Phase 4 - Liftoff Phase 5 - Powered Ascent Phase 6 - Unpowered Ascent
Failure To Detonate At Decoupling Event Altitude	Power Loss. Wire severance due to high acceleration speeds. Bad e-match.	Medium	Backup detonation timer.Software outputs continues detonation command rather than one-time event. Output voltage for detonation is highest rating for e-matches.Multiple ematches connected to several end-circuit detonation devices.	Low	Avionics	Phase 7 - Drogue deployment and controlled descent
Loss Of Data	Loss of communication with rocket.	Medium	Data is logged to internal memory of GPS module. Memory is independently powered.	Low	Avionics	Phase 5 - Powered Ascent Phase 6 - Unpowered Ascent Phase 7 - Drogue deployment and controlled descent Phase 10 - Main Deployment
Loss Of Communication With Rocket	Discrepancy in communication module	Medium	Extensive testing and case handling for all potential communication string errors	Medium	Avionics	
	Damage from cosmic radiation	Medium	Multiple redundancies on board	Low	Avionics	
Loss Of Rocket Position	GPS Failure Altimeter Failure IMU Failure	Medium	Chances of all these sensors failing simultaneously is extremely low. Positional data and altitude can be extrapolated from any one of these sensors. These calculations will be done internally and only called if the others become unresponsive.	Low	Avionics	

Appendix 5: Assembly, Preflight and Launch Operations Checklists

McGill Rocket Team's procedures are divided into operations/integration checklists and subteam-specific assembly checklists. Furthermore, the operations checklists are subdivided into nominal, contingency and emergency procedures and cover every stage from pre-flight assembly to recovery. Finally, there are final pre-flight verification sheets to be reviewed by the team launch manager before the rocket is presented to the competition officials and brought out to the launch pad.

MRT Operations Checklist - Nominal Procedures

Project Caladan | May 2019

Step	Division	Task	Complete
1.0		PRE-FLIGHT AREA ASSEMBLY - RECOVERY	
1.1	Recovery	Pack main parachute in deployment bag	☐
1.2	Recovery	Fold drogue and wrap in nomex blanket	☐
1.3	Recovery	Ensure all shock cords are z-folded	☐
1.4	Recovery	Attach e-matches to tender descender	☐
1.5	Recovery	Verify all components of recovery mechanism are accounted for	☐
2.0		PRE-FLIGHT AREA ASSEMBLY - AVIONICS BAY	
2.1	Avionics	Assemble AV bays as per AVIONICS checklist.	☐
2.2	Avionics	Make sure main power switches are turned off.	☐
2.3	Avionics	Visually verify all main power connections.	☐
2.4	Avionics	Connect e-matches to screw terminals	☐
3.0		PRE-FLIGHT AREA ASSEMBLY - NOSE CONE	
3.1	Payload	Assembly payload as per PAYLOAD checklist.	☐
3.2	Payload	Verify payload assembly is properly prepared.	☐
3.3	Payload	Ensure tubing is properly sealed by pinch valve.	☐
3.4	Payload	Insert payload "wedding cake" assembly into nose cone.	☐
3.5	Structure	Screw nose-cone tip onto protruding threaded rod.	☐
3.6	Structure	Ensure nose cone assembly integrity is suffciently tight/robust.	☐
4.0		PRE-FLIGHT AREA ASSEMBLY - MOTOR	
4.1	Propulsion	Obtain motor, spacer, e-matches from vendor and verify components.	☐
4.2	Propulsion	Grease motor casing and threads on motor casing with silicone spray.	☐
4.3	Propulsion	Assemble motor as per manufacturer instructions.	☐
4.4	Propulsion	Allow glued grains to cure for 24h.	☐
5.0		FLIGHT AREA - AVIONICS BAY	
5.1	Avionics	Assemble AV bay as per avionics assembly checklist.	☐
5.2	Avionics	Screw in AV bay to engine block.	☐
5.3	Structure	Insert and align coupler piece with patch antenna glued into bottom body tube.	☐
5.4	Avionics	Connect ejection wires to bulkhead.	☐
5.5	Avionics	Connect patch antenna to AV bay.	☐
5.6	Avionics	Turn on avionics and verify circuit continuity.	☐
5.7	Structure	Join body tubes and insert screws.	☐
6.0		FLIGHT AREA - RECOVERY	
6.1	Recovery	Load black powder in tender descenders and secure with plastic screws	☐
6.2	Recovery	Load black powder into charge wells	☐
6.3	Recovery	Assemble recovery mechanism as per RECOVERY checklist	☐

6.4	Recovery	Verify the recovery mechanism is properly assembled	☐
6.5	Structure	Attach upper body tube to top coupler	☐
6.6	Payload	Activate payload electronics	☐
6.7	Structure	Secure nosecone using shear pins	☐
7.0		FLIGHT AREA - PROPULSION	
7.1	Propulsion	Load engine in place	☐
7.2	Propulsion	Screw retaining cap in place	☐
7.3	Propulsion	Wind igniter around supporting stick.	☐
7.4	Propulsion	Prepare spare igniter in same fashion.	☐
8.0		PREFLIGHT CHECKLIST	
8.1	N/A	Carry rocket and igniters out to launch pad.	☐
8.2	N/A	Install rocket on rail.	☐
8.3	N/A	Set launch angle on rail.	☐
8.4	Avionics	Arm - flip switches and press push buttons.	☐
8.5	Avionics	Listen for proper beep sequence and active telemetry.	☐
8.6	Propulsion	Install engine igniter.	☐
8.7	Propulsion	Verify continuity on motor igniter.	☐
8.8	All	Evacuate launch area to designated location.	☐
9.0		LAUNCH CHECKLIST	
9.1	N/A	In event of launch abort or hang fire, proceed to CONTINGENCY 3.0/4.0, respectively.	☐
9.2	Propulsion	Ignite motor.	☐
9.3	All	Track rocket through telemetry and visual aid.	☐
9.4		If flight is off-nominal, proceed to CONTINGENCY 5.0-9.0, depending on specific case.	☐
10.0		RECOVERY CHECKLIST	
10.1	Avionics	If arming lock is still in tact and it is possible to do so, disarm - flip switches and press push buttons to disarm circuitry.	☐
10.2	Payload	Check if nose cone is structurally intact.	☐
10.3	Payload	Remove payload from nose cone.	☐
10.4	Payload	Clamp payload tubes around cassettes.	☐
10.5	Payload	Cut out tubes with the clamped cassettes and extract from nose cone assembly.	☐
10.6	Payload	Place cassettes, with clamped tubes, in sterilised bags.	☐
10.7	Payload	Store samples in specially prepared, insulated, container.	☐
10.8	Payload	Secure container so that it will not be opened accidentally.	☐
10.9	All	Gather all nearby pieces of rocket and reassemble it in a form suitable for transportation.	☐
11.0	All	Return rocket to base camp.	☐
11.1	Payload	Seal ends of clamped tubes with vulcanizing silicone.	☐
11.2	Payload	Store samples in cooler, for return to McGill for analysis.	☐

MRT Operations Checklist - Contingency Procedures

Project Caladan May 2019

Step	Division	Task	Complete
1.0		ASSEMBLY - CIRCUIT BOARD SHORT	
1.1	Avionics	Disconnect boards to prevent further damage.	☐
1.2	Avionics	Retrieve spare AV bay assembly from storage.	☐
1.3	Avionics	Assemble as per the AVIONICS checklist.	☐
1.4	Avionics	Proceed with NOMINAL 5.0.	☐
2.0		FLIGHT AREA - PREMATURE EJECTION	
2.1	Avionics	Make sure main power switches are turned off.	☐
2.2	Avionics	Visually verify all main power connections	☐
2.3	Avionics	Connect e-matches to screw terminals	☐
3.0		LAUNCH - LAUNCH ABORT	
3.1	N/A	Await permission to approach rocket.	☐
3.2	Propulsion	Disconnect igniter and remove from rocket.	☐
3.3	Avionics	Disarm energetics by pressing rocket switches/push buttons.	☐
3.4	All	Bring down launch rail and slide rocket out of rail.	☐
3.5	All	Return rocket to base camp.	☐
4.0		LAUNCH - HANG FIRE	
4.1	N/A	Attempt to relight the motor twice, following official instructions.	☐
4.2	Propulsion	Wait until given permission to approach rocket.	☐
4.3	Propulsion	Remove spent igniter, insert spare pre-assembled igniter piece.	☐
4.4	Propulsion	Retreat from launch area, go to NOMINAL 9.0	☐
5.0		CATO	
5.1	All	Take shelter from possible incoming debris.	☐
5.2	All	Obtain authorization from competition officials before approaching.	☐
5.3	Propulsion	Locate motor casing before approaching rocket pieces.	☐
5.4	All	Verify that grains have fully burnt out and that motor block is safe to approach.	☐
5.5	All	Identify avionics bay, if still intact.	☐
5.6	All	If AV bay is still intact, disarm electronics before proceeding.	☐
5.7	All	Gather as many parts as feasible for post-mortem analysis	☐
6.0		OFF-NOMINAL - FLIGHT PROFILE DEVIATION	
6.1	Structure	Slide AV skin over the bay	☐
6.2	Stucture	Screw the AV skin in place	☐
6.3	Avionics	Insert all circuit breaker pins	☐
6.4	Avionics	Activate main power switches	☐
6.5	Avionics	Verify functioning telemetry	☐

7.0		OFF-NOMINAL - BALLISTIC DESCENT	
7.1	Recovery	Load black powder in TD's and secure with plastic screws	☐
7.2	Recovery	Load black powder into charge wells	☐
7.3	Recovery	Assemble recovery mechanism as per recovery mechanism procedure	☐
7.4	Assembler	Verify the recovery mechanism is properly assembled	☐
7.5	Structure	Attach upper body tube to top coupler	☐
7.6	Payload	Activate payload electronics	☐
	Structure	Secure nosecone using shear pins	☐

8.0		OFF-NOMINAL - NO MAIN	
8.1	N/A	Avoid approaching top half of rocket before disarming electronics.	☐
8.2	N/A	Proceed to NOMINAL 10.0	☐

9.0		LOSS OF TELEMETRY	
9.1	N/A	Follow checklist until position of rocket is acquired - then proceed to NOMINAL 10.0	
9.2	Avionics	Loudly announce loss of telemetry to team.	☐
9.3	All	Attempt to obtain visual confirmation of rocket.	☐
9.4	Avionics	Move yagi antenna to higher ground, such as from launch tower.	☐
9.5	Avionics	Drive out to cell signal with IRIDIUM phone.	☐
9.6	Avionics	Await message from Iridium network.	☐

MRT Operations Checklist - Emergency Procedures

Project Caladan May 2019

Step	Division	Task	Complete
1.0		INJURY TO PERSONNEL	
1.1	All	Ensure there are no active threats or hazards before approaching.	☐
1.2	All	If area could become dangerous, move injured person to safe area.	☐
1.3	All	Apply first aid or fetch first-aid trained person.	☐
1.4	All	Immediately notify competition officials and medical tent.	☐
1.5	All	Depending on injury severity, locate personnel with cell service and call 911.	☐
2.0		PERSONNEL HEAT STROKE	
2.1	All	Recognize symptoms of heat stroke: confusion, agitation, slurred speech, nausea, flushed skin, rapid breathing, rapid heartbeat, headache, hot and dry skin (no sweat)	☐
2.2	All	If available, immediately notify medical tent. Otherwise, call 911 or locate personnel with cell service.	☐
2.3	All	Move affected person to shade.	☐
2.4	All	Remove excess clothing.	☐
2.5	All	Sponge with cool water, apply cold towels.	☐
2.6	All	Give only cool water to drink.	☐
3.0		PERSONNEL ILLNESS	
3.1	All	Recognize personnel in distress. Identify and vocalize if own body is feeling abnormal.	☐
3.2	All	Bring affected person to shade.	☐
3.3	All	Give only cool water to drink.	☐
3.4	All	Immediately notify medical tent.	☐
4.0		FIRE	
4.1	All	Immediately evacuate area.	☐
4.2	All	Notify competition officials.	☐
4.3	All	If deemed safe to approach, attempt to extinguish with fire extinguisher.	☐

MRT Avionics Assembly Checklist

Project Caladan May 2019

Step	Division	Task	Complete
1.0		PRE-FLIGHT AREA ASSEMBLY - ELECTRONICS	
1.1	Avionics	Insert batteries into battery casing	☐
1.2	Avionics	Ensure horizontal PCBs are secured to horizontal braces	☐
1.3	Avionics	Insert switches into switch brace	☐
1.4	Avionics	Slide vertical PCBs into vertical brace	☐
1.5	Avionics	Ensure secure connection between all electronics and braces	☐
2.0		PRE-FLIGHT AREA ASSEMBLY - AVIONICS BAY STRUCTURE	
2.1	Avionics	Thread nylon rods into top engine block	☐
2.2	Avionics	Slide battery casing, with batteries, onto rods	☐
2.3	Avionics	Slide horizontal braces (3) onto rods on top of battery casing	☐
2.4	Avionics	Slide power switch brace onto rods	☐
2.5	Avionics	Slide final horizontal braces (2) onto rods on top of battery casing	☐
2.6	Avionics	Slide vertical brace (1) onto rods on top of horizontal braces	☐
2.7	Avionics	Insert top-most brace onto the stack	☐
2.8	Avionics	Insert nuts and washers onto rods to secure structure	☐
3.0		PRE-FLIGHT AREA ASSEMBLY - WIRING	
3.1	Avionics	Connect power switches to Battery Input Board	☐
3.2	Avionics	Connect Battery Input Board to Power Board 1	☐
3.3	Avionics	Verify polarity of connection, Green LED indicates properly connected when powered	☐
3.4	Avionics	Connect Battery Input Board to Power Board 2	☐
3.5	Avionics	Verify polarity of connection, Green LED indicates properly connected when powered	☐
3.6	Avionics	Plug ouput of Power Board 1 to Output Bus	☐
3.7	Avionics	Verify Polarity match between Power Boards by visually identifying wire colors	☐
3.8	Avionics	Connect Output Bus to Ejection circuit	☐
3.9	Avionics	Verify polarity (Green LED means nomimal)	☐
4.0	Avionics	Connect Ouput Bus to GPS Redundancy	☐
4.1	Avionics	Connect Output Bus to Telemetry	☐
4.2	Avionics	Connect E-Match Board to Ejection Circuits	☐

MRT Recovery Assembly Checklist

Project Caladan — May 2019

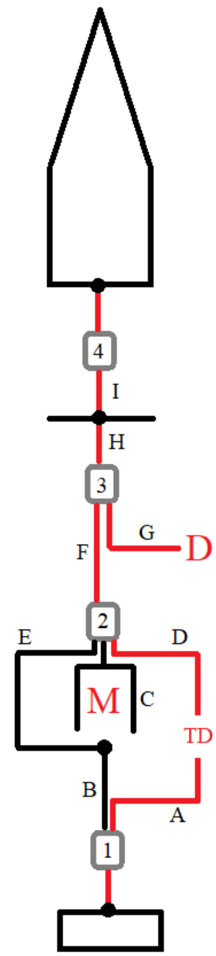

Step	Division	Task	Complete
1.0		PRE-FLIGHT AREA ASSEMBLY - RECOVERY PACKING	
1.1	Recovery	Z-fold main parachute canopy	☐
1.2	Recovery	Make sure that the slider ring is in place	☐
1.3	Recovery	Pack the main parachute into the deployment bag and secure the lines	☐
1.4	Recovery	Z-fold all shock cords and secure in bundles using masking tape	☐
1.5	Recovery	Verify all components of recovery mechanism are accounted for	☐
2.0		FLIGHT AREA - TENDER DESCENDERS PREPARATION	
2.1	Recovery	Load black powder into tender descenders	☐
2.2	Recovery	Connect e-matches	☐
2.3	Recovery	Close the tender descenders around the shock cords	☐
2.4	Recovery	Secure with nylon screws	☐
3.0		FLIGHT AREA - CHARGE WELLS PREPARATION	
3.1	Recovery	Load black powder into glove fingers	☐
3.2	Recovery	Connect e-matches	☐
3.3	Recovery	Secure bundles with masking tape and place into the charge wells	☐
3.4	Recovery	Put on the silicone cap and secure with silicone tape	☐
3.5	Recovery	Pass wire through the plate hole and guiding straws	☐
4.0		FLIGHT AREA - RECOVERY PACKING	
4.1	Recovery	Connect quick links 1 and 4 to base shock cords	☐
4.2	Recovery	Connect cords A and B to quick link 1	☐
4.3	Recovery	Tighten quick link 1 and secure cords in place with masking tape	☐
4.4	Recovery	Connect cords D, C, and E to quick link 2	☐
4.5	Recovery	Connect cord F to quick link 2	☐
4.6	Recovery	Tighten quick link 2 and secure cords in place with masking tape	☐
4.7	Recovery	Connect cords F and G to quick link 3	☐
4.8	Recovery	Connect cord H to quick link 3	☐
4.9	Recovery	Tighten quick link 3 and secure cords in place with masking tape	☐
5.0	Recovery	Connect cord I to quick link 4	☐
5.1	Recovery	Tighten quick link 4 and secure cords in place with masking tape	☐
5.2	Recovery	Fold nomex blanket around drogue parachute	☐
5.3	Recovery	Push all recovery components into the body tube	☐
5.4	Recovery	Ensure that the free plate is placed properly against the coupler ring	☐
6.0		FLIGHT AREA - CLOSING	
6.1	Recovery	Align and close the nose cone	☐
6.2	Recovery	Screw in nylon screws	☐
6.3	Recovery	Align and close the bottom tube	☐
6.4	Recovery	Screw in steel screws	☐

MRT Payload Assembly Checklist

Project Caladan May 2019

Step	Division	Task	Complete
1.0		PRE-FLIGHT AREA ASSEMBLY - PAYLOAD ELECTRONICS	
1.1		Ensure that both batteries are fully charged	☐
1.2	Payload	Connect sensors, MOSFETs, valves to Teensy	☐
1.3	Payload	Upload code to Teensy	☐
1.4	Payload	Ensure SD card is in the Teesny	☐
1.5	Payload	Ensure all connections are on the correct pins	☐
1.6	Payload	Attach batteries to system (dedicated cables implemented already)	☐
1.7	Payload	Verify that all electronics components are accounted for and working	☐
2.0		PRE-FLIGHT AREA ASSEMBLY - PAYLOAD SAMPLING MECHANISM (AT LAB)	
2.1	Payload	Ensure that all respective elements have been sterilized by ethanol and are now dry	☐
2.2	Payload	Attach tubing to cassettes, and all connecting pieces to tubing (form plumbing diagram)	☐
2.3	Payload	Place filters in cassettes	☐
2.4	Payload	Place clamps at end of tubing to seal cassettes	☐
2.5	Payload	Attach tubing to pumps	☐
2.6	Payload	Apply pinch valve to tubing	☐
2.7	Payload	Connect pumps to MOSFETS	☐
3.0		PRE-FLIGHT AREA ASSEMBLY - WEDDING CAKE STRUCTURE AND INTEGRATION	
3.1	Payload	Place all enclosed parts (batteries, pumps, etc.) in their enclosures	☐
3.2	Payload	Place enclusores onto the proper rods, secure with nuts	☐
3.3	Payload	Screw all rods and plates together and secure	☐
3.4	Payload	Attach pumps to tubing	☐
3.5	Payload	Attach pumps to battery	☐
3.6	Payload	Complete rest of tubing plumbing	☐
3.7	Payload	Connect electronics system to battery	☐
3.8	Payload	Ensure that the structure is properly secured, all components accounted for	☐

Appendix 6: Engineering Drawings

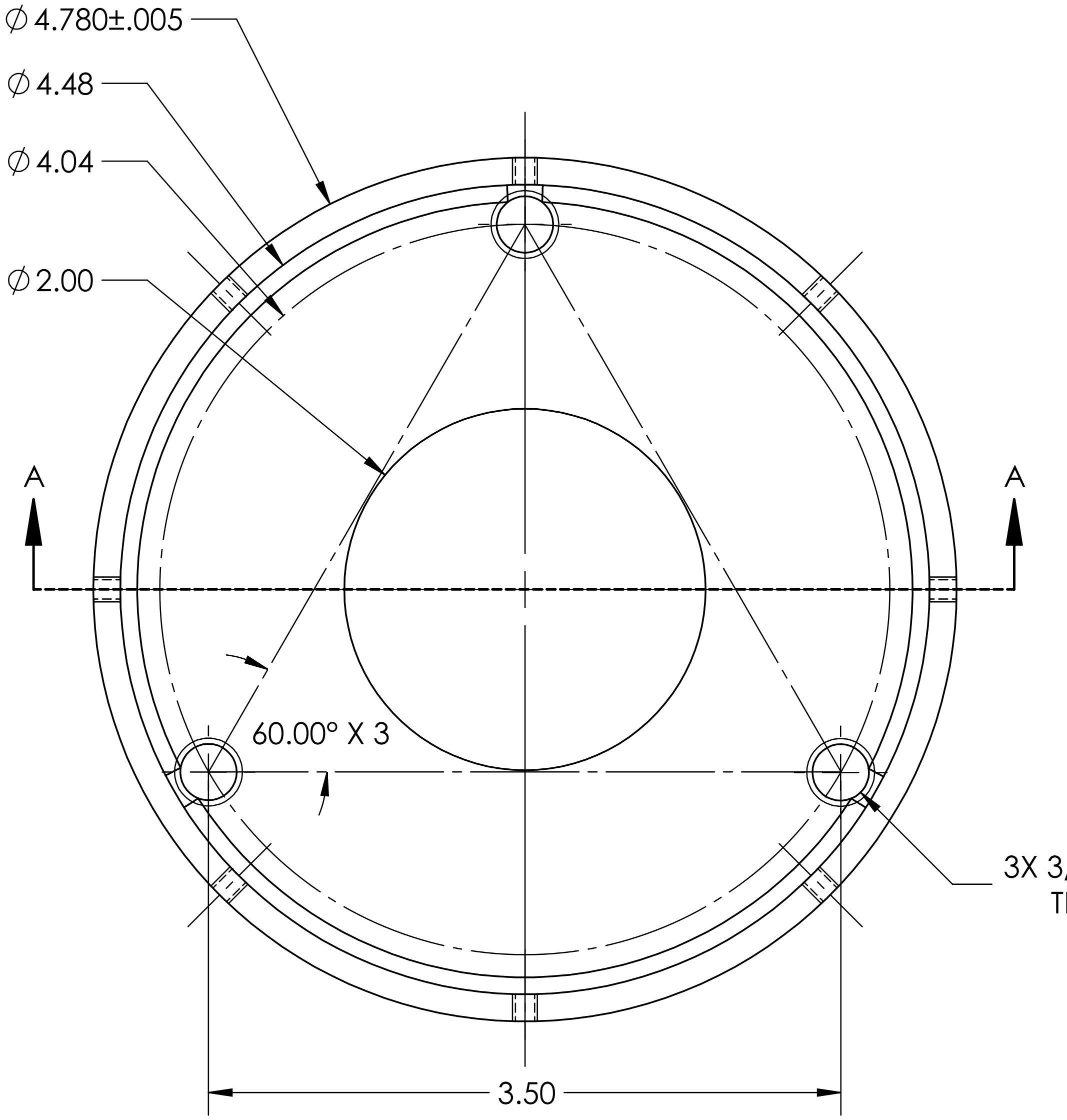

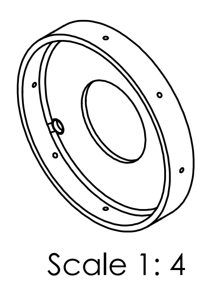

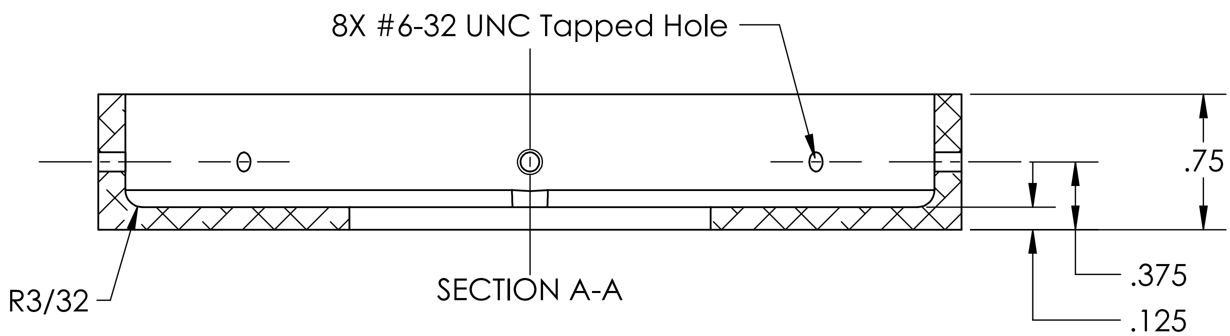

REFERENCE FILE: Caladan_TopBlock				QUANTITY 1
ENGLISH DIMENSIONS IN INCHES	SCALE: 1:1	DRAWN BY ANTOINE MERCIER	DATE 02.03.19	APPROVED NR 03.03.19
GENERAL TOLERANCES LINEAR: ±0.01 ANGULAR: ±0.5°		MRT	3480 UNIVERSITY ST. MONTREAL, QC, H3A 0E9 CANADA www.mcgillrocketteam.com	
SURFACE TEXTURE -		MODEL NAME CALADAN TOP ENGINE BLOCK		
MATERIAL Al 6061 T6		DRAWING NO. 1		SHEET 1 OF 1

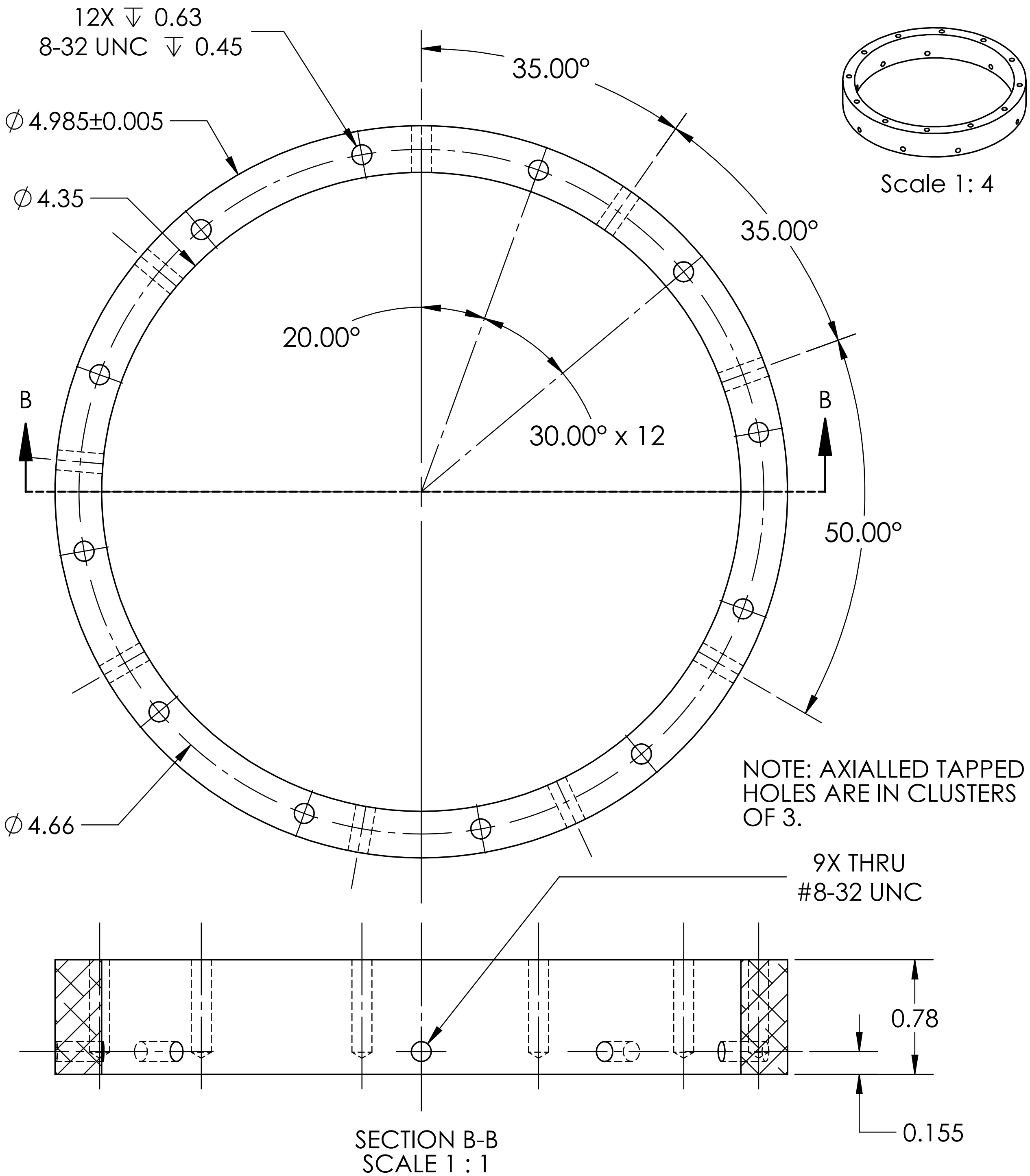

REFERENCE FILE: Caladan_BottomBlock				QUANTITY 1
ENGLISH DIMENSIONS IN INCHES	SCALE: 1:1	DRAWN BY ANTOINE MERCIER	DATE 02.03.19	APPROVED NR 03.03.19
GENERAL TOLERANCES LINEAR: ±0.01 ANGULAR: ±0.5°		MRT	3480 UNIVERSITY ST. MONTREAL, QC, H3A 0E9 CANADA www.mcgillrocketteam.com	
SURFACE TEXTURE -		MODEL NAME CALADAN BOTTOM ENGINE RETAINER		
MATERIAL Al 6061 T6		DRAWING NO. 1		SHEET 1 OF 1

ITEM NO.	PART	QTY.
1	BATTERY CASING	1
2	HORIZONTAL BRACE	5
3	SWITCH BRACE	1
4	VERTICAL BRACE	1
5	BRACE CAP	1
6	3/8 - 32 NUT	6
7	3/8 - 32 NYLON ROD	3

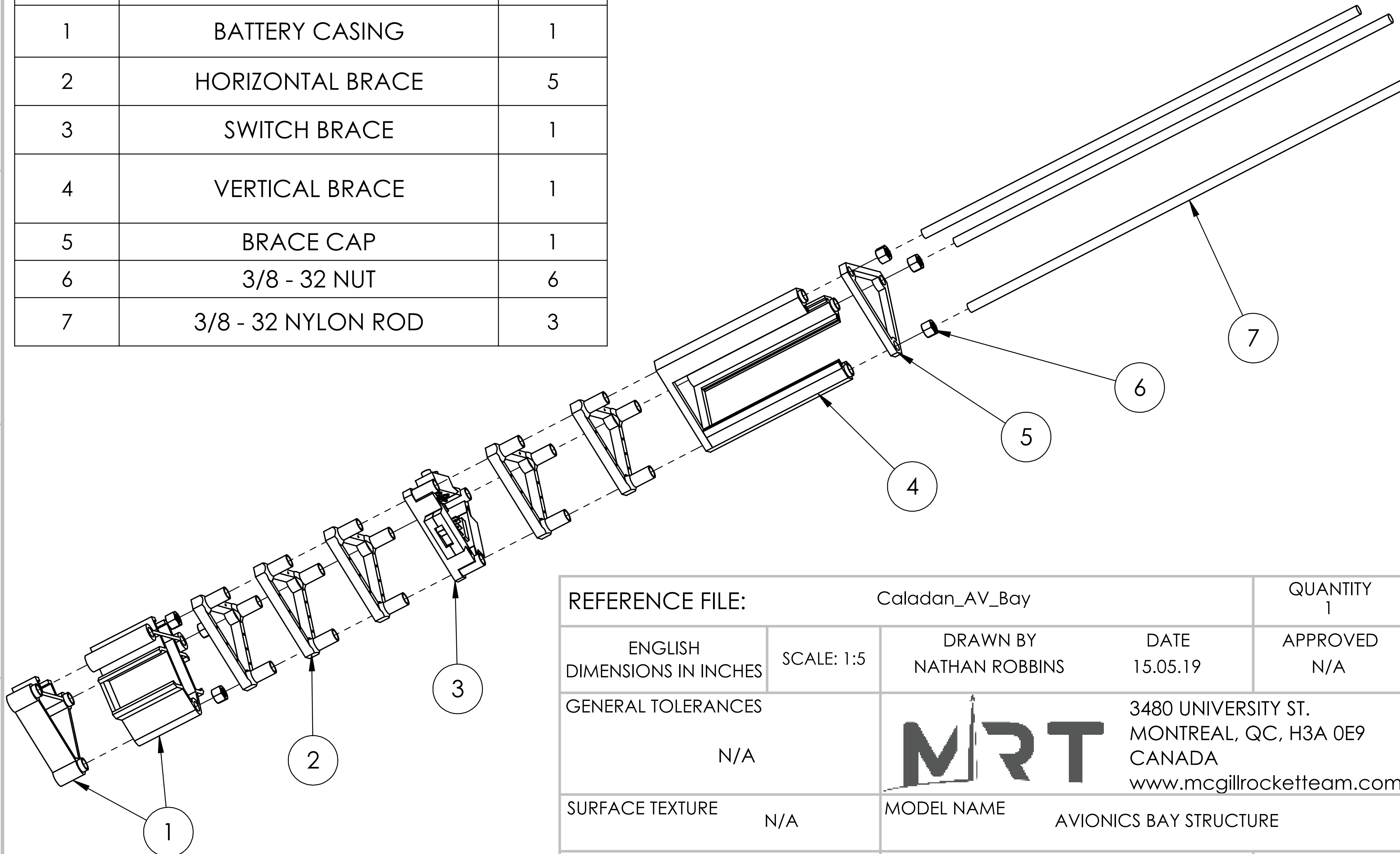

REFERENCE FILE:	Caladan_AV_Bay		QUANTITY 1
ENGLISH DIMENSIONS IN INCHES	SCALE: 1:5	DRAWN BY NATHAN ROBBINS / DATE 15.05.19	APPROVED N/A
GENERAL TOLERANCES N/A		3480 UNIVERSITY ST. MONTREAL, QC, H3A 0E9 CANADA www.mcgillrocketteam.com	
SURFACE TEXTURE N/A		MODEL NAME AVIONICS BAY STRUCTURE	
MATERIAL N/A		DRAWING NO. 1	SHEET 1 OF 1

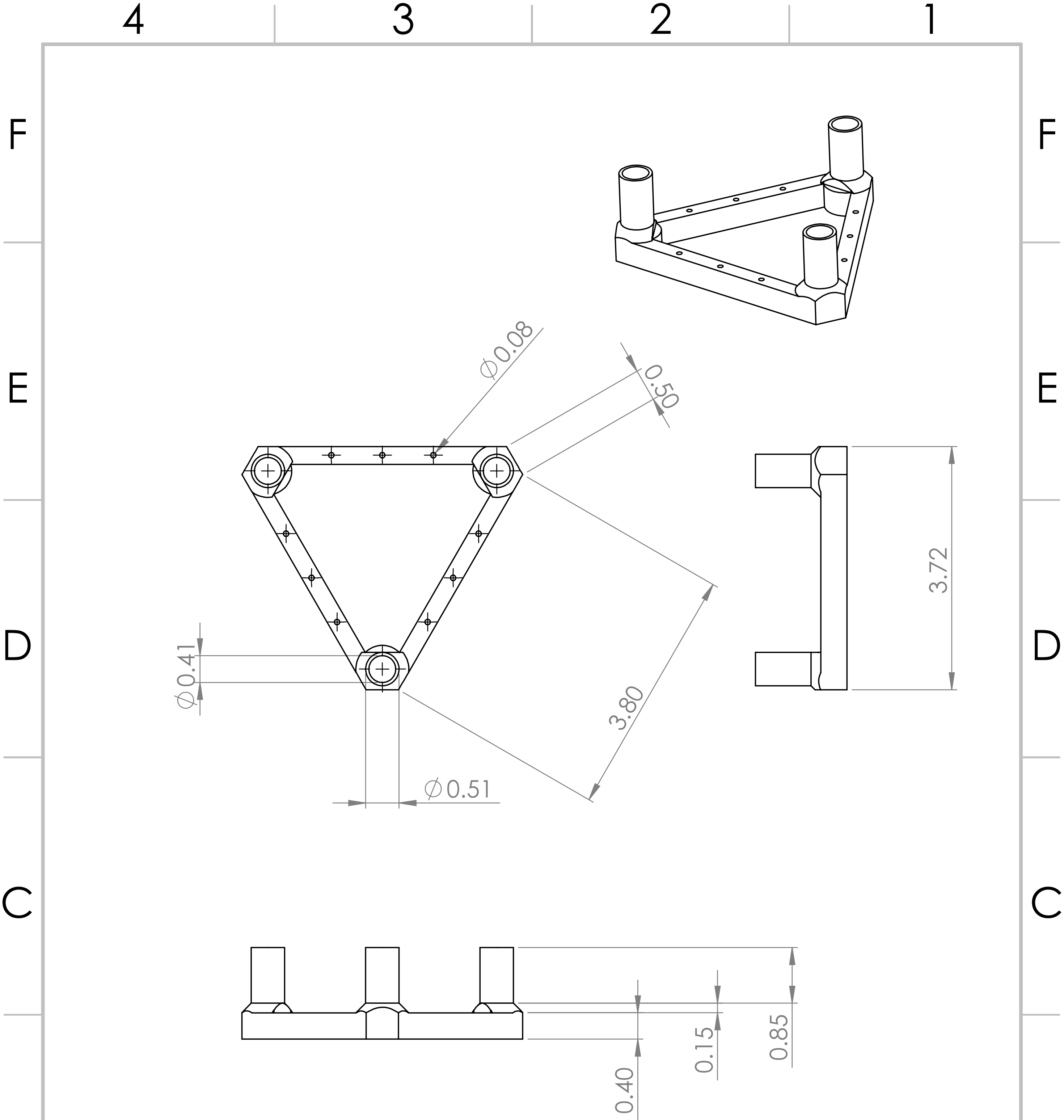

REFERENCE FILE: 3-1_Base_Brace				QUANTITY 5
ENGLISH DIMENSIONS IN INCHES	SCALE: 1:2	DRAWN BY Liem Dam-Quang	DATE 16.05.19	APPROVED N/A
GENERAL TOLERANCES 1 DECIMAL ±0.1 2 DECIMAL ±0.01 3 DECIMAL ±0.002		MRT	3480 UNIVERSITY ST. MONTREAL, QC, H3A 0E9 CANADA www.mcgillrocketteam.com	
SURFACE TEXTURE -		MODEL NAME PCB Brace		
MATERIAL PETG		DRAWING NO. 1		SHEET 1 OF 1

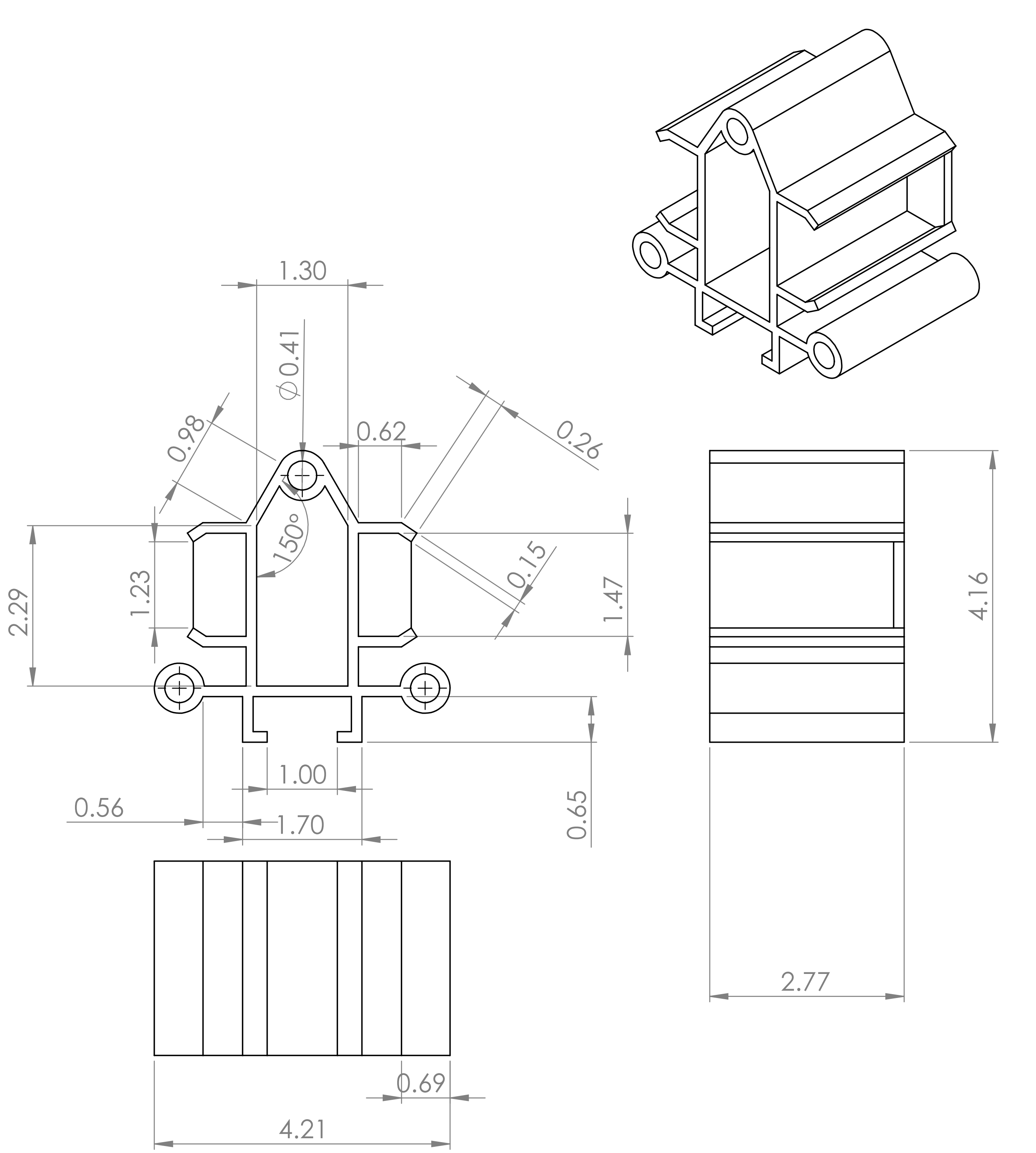

REFERENCE FILE:	BatteryCasingTop			QUANTITY 1
ENGLISH DIMENSIONS IN INCHES	SCALE: 1:2	DRAWN BY Liem Dam-Quang	DATE 16.05.19	APPROVED N/A
GENERAL TOLERANCES 1 DECIMAL ±0.1 2 DECIMAL ±0.01 3 DECIMAL ±0.002		MRT	3480 UNIVERSITY ST. MONTREAL, QC, H3A 0E9 CANADA www.mcgillrocketteam.com	
SURFACE TEXTURE N/A		MODEL NAME Battery Casing Top		
MATERIAL PETG		DRAWING NO. 1		SHEET 1 OF 1

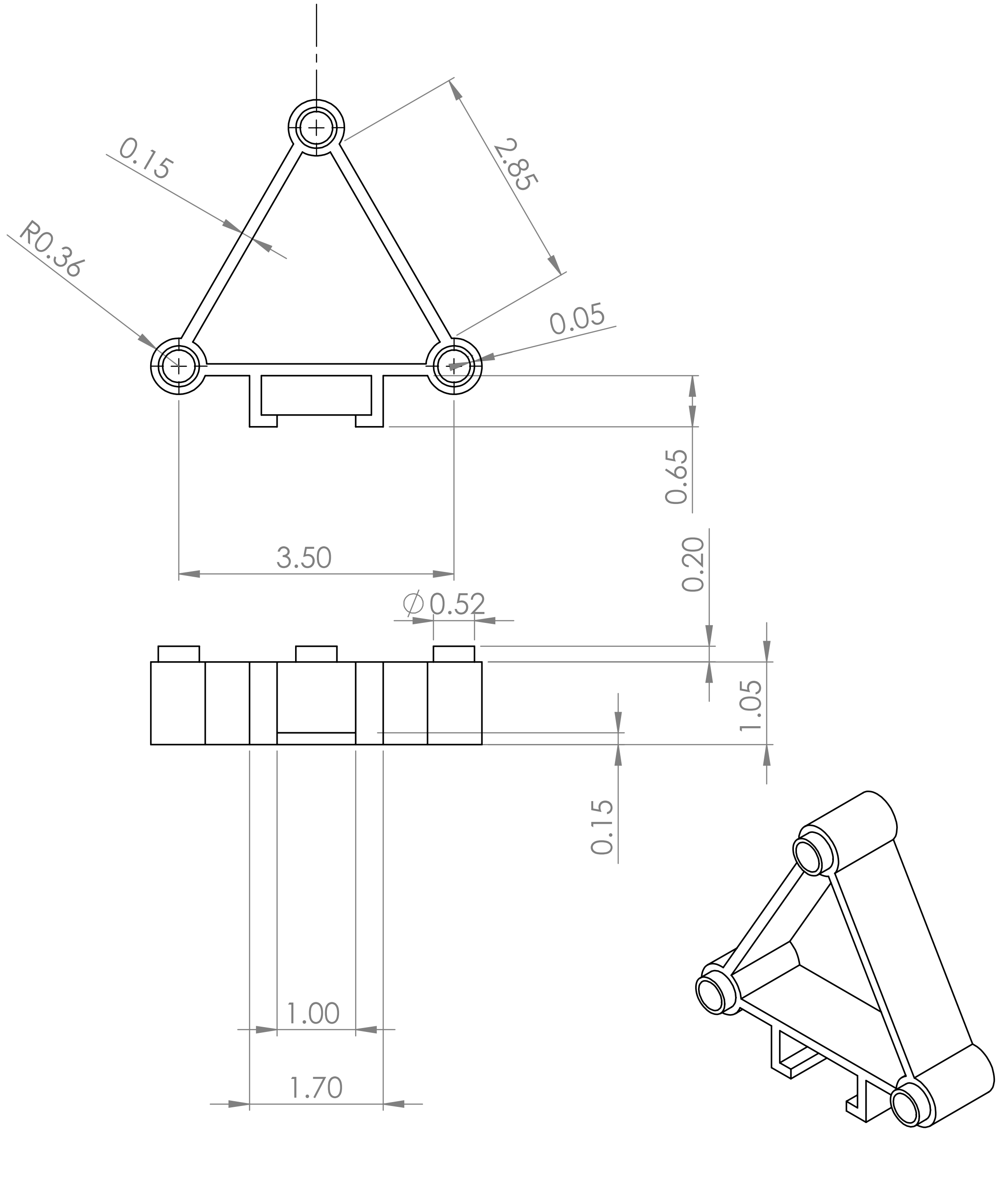

REFERENCE FILE: BatteryCasingBottom				QUANTITY 1
ENGLISH DIMENSIONS IN INCHES	SCALE: 1:2	DRAWN BY Liem Dam-Quang	DATE 16.05.19	APPROVED N/A
GENERAL TOLERANCES 1 DECIMAL ±0.1 2 DECIMAL ±0.01 3 DECIMAL ±0.002		MRT	3480 UNIVERSITY ST. MONTREAL, QC, H3A 0E9 CANADA www.mcgillrocketteam.com	
SURFACE TEXTURE N/A		MODEL NAME Battery Casing Bottom		
MATERIAL PETG		DRAWING NO. 1		SHEET 1 OF 1

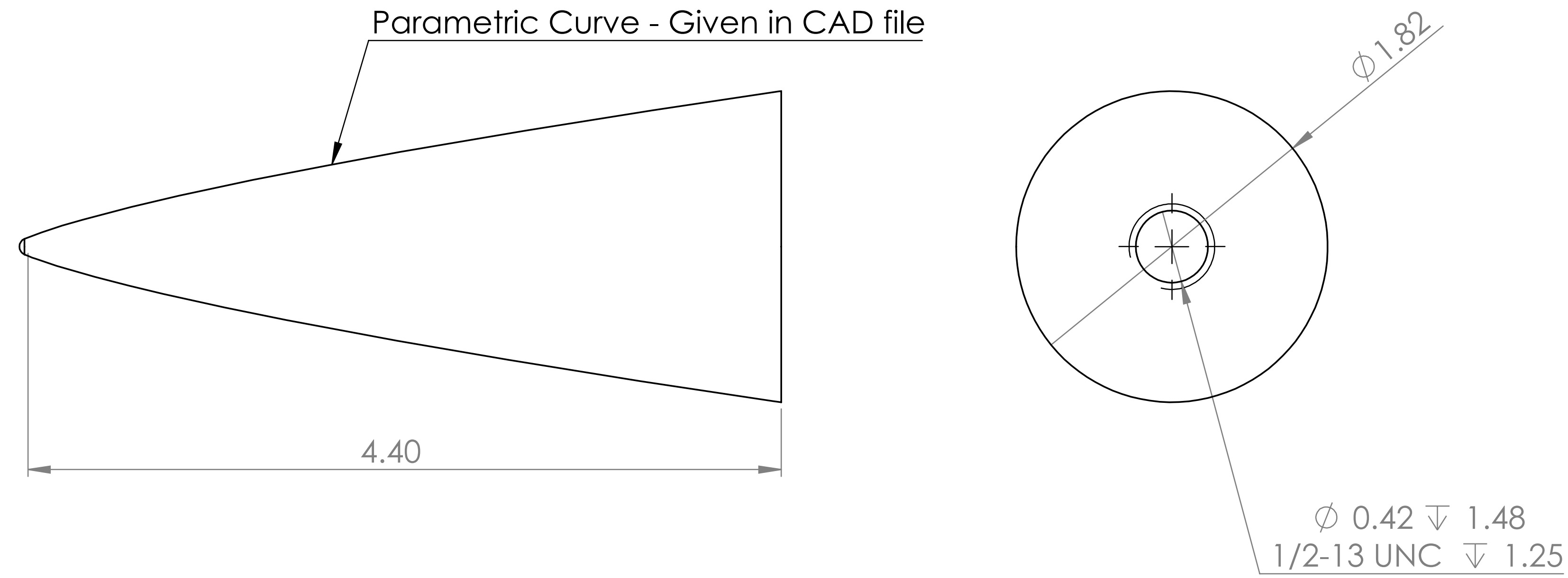

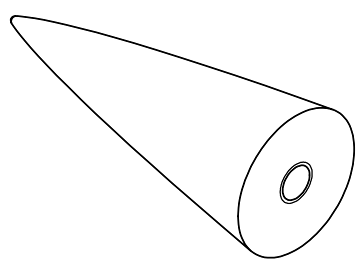

REFERENCE FILE:		NC_Tip		QUANTITY 1
ENGLISH DIMENSIONS IN INCHES	SCALE: 1:1	DRAWN BY CAMILLE RICHER	DATE	APPROVED J O-L 03.03.19
GENERAL TOLERANCES 1 DECIMAL ±0.1 2 DECIMAL ±0.01 3 DECIMAL ±0.002		MRT	3480 UNIVERSITY ST. MONTREAL, QC, H3A 0E9 CANADA www.mcgillrocketteam.com	
SURFACE TEXTURE		MODEL NAME NOSE CONE TIP		
MATERIAL Al 6061 T6		DRAWING NO. 1		SHEET 1 OF 1

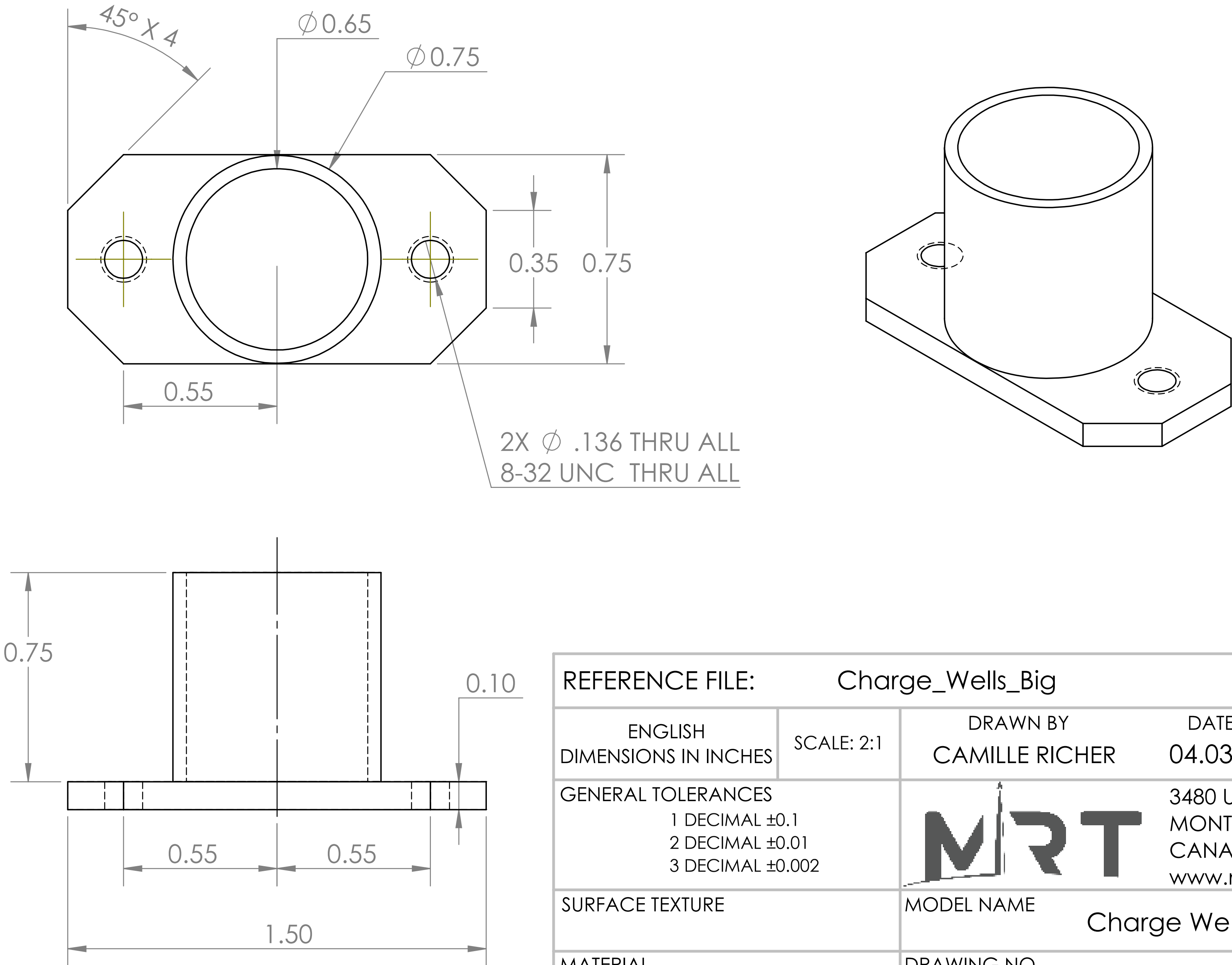

REFERENCE FILE: Charge_Wells_Big				QUANTITY 2
ENGLISH DIMENSIONS IN INCHES	SCALE: 2:1	DRAWN BY CAMILLE RICHER	DATE 04.03.19	APPROVED JL 06.03.19
GENERAL TOLERANCES 1 DECIMAL ±0.1 2 DECIMAL ±0.01 3 DECIMAL ±0.002		MRT	3480 UNIVERSITY ST. MONTREAL, QC, H3A 0E9 CANADA www.mcgillrocketteam.com	
SURFACE TEXTURE		MODEL NAME Charge Well - Large		
MATERIAL Al 6061 T6		DRAWING NO. 1		SHEET 1 OF 1

#	Name	Material
1	Bottom Plate	Carbon Fiber
2	Air Inlet	Steel
3	Valve Enclosure	PTG
4	Sterile Cassettes	-
5	First Mid-Plate	6061 T6
6	Valve Enclosure x2	PTG
7	Second Mid-Plate	6061 T6
8	Electronics	-
9	Top plate	1045 Steel
10	Battery Enclosure	PTG

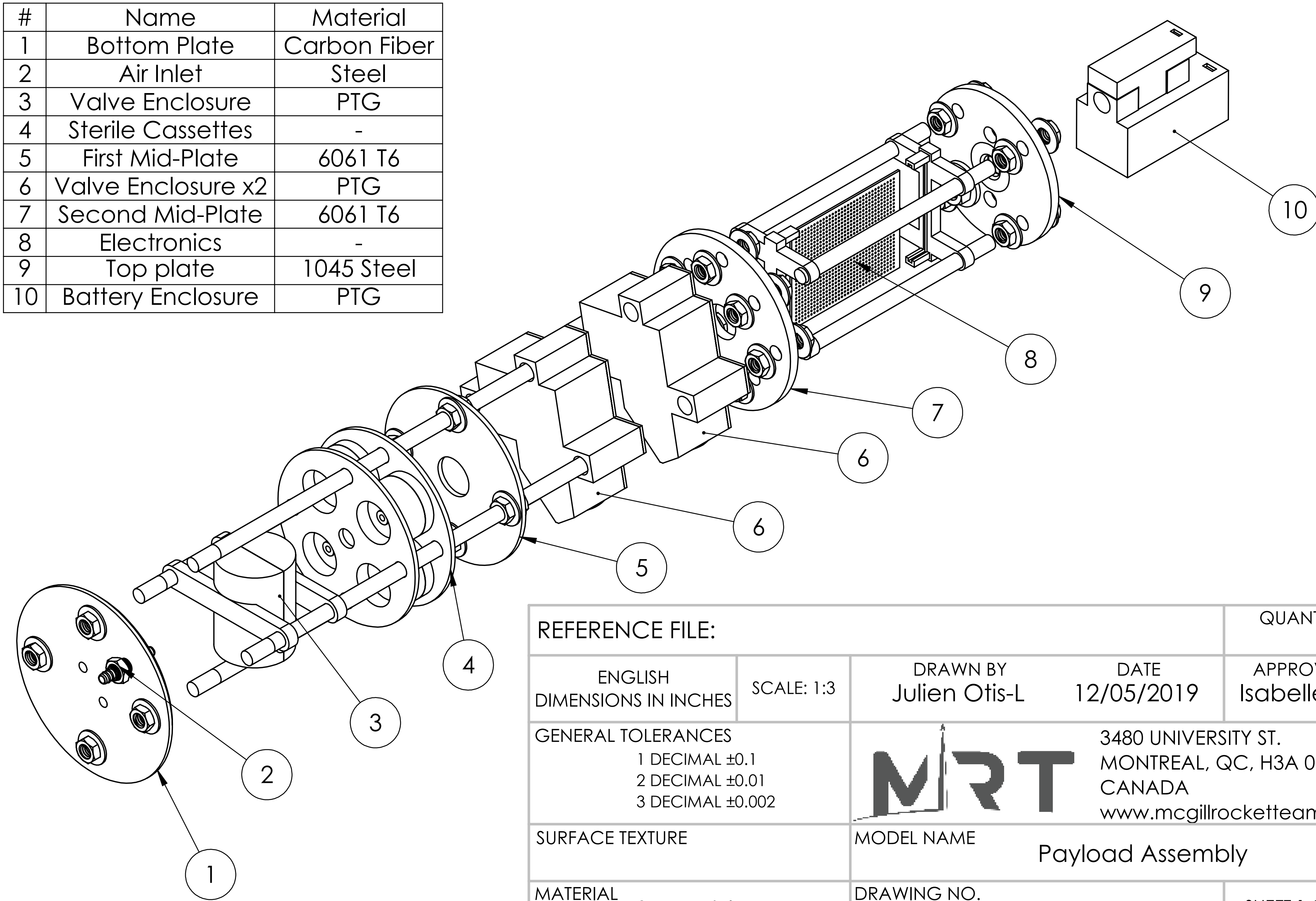

REFERENCE FILE:				QUANTITY
ENGLISH DIMENSIONS IN INCHES	SCALE: 1:3	DRAWN BY Julien Otis-L	DATE 12/05/2019	APPROVED Isabelle P-A
GENERAL TOLERANCES 1 DECIMAL ±0.1 2 DECIMAL ±0.01 3 DECIMAL ±0.002		MRT 3480 UNIVERSITY ST. MONTREAL, QC, H3A 0E9 CANADA www.mcgillrocketteam.com		
SURFACE TEXTURE		MODEL NAME Payload Assembly		
MATERIAL See Table		DRAWING NO. 1		SHEET 1 OF 1

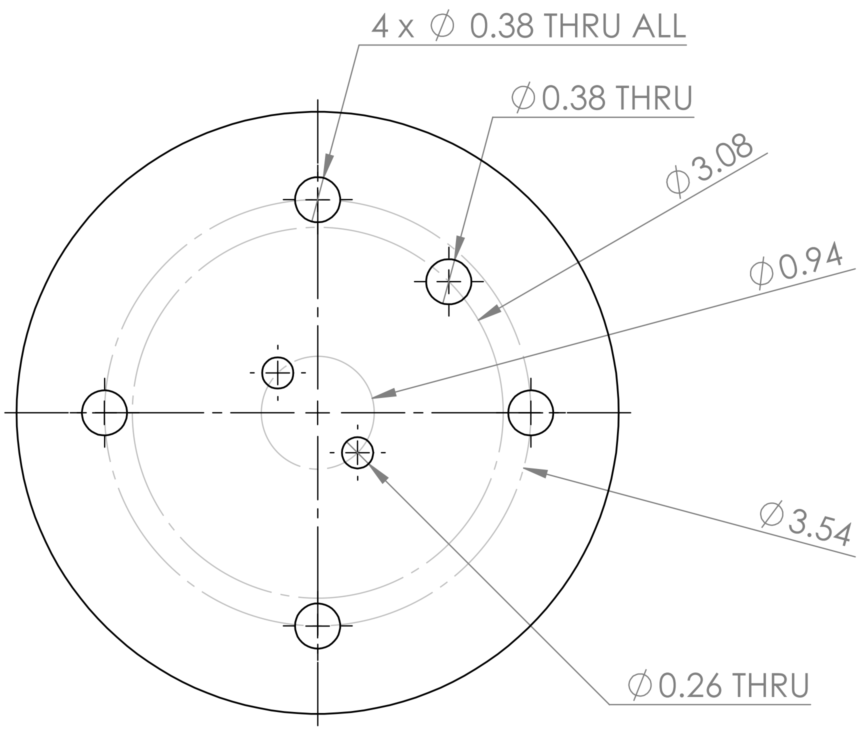

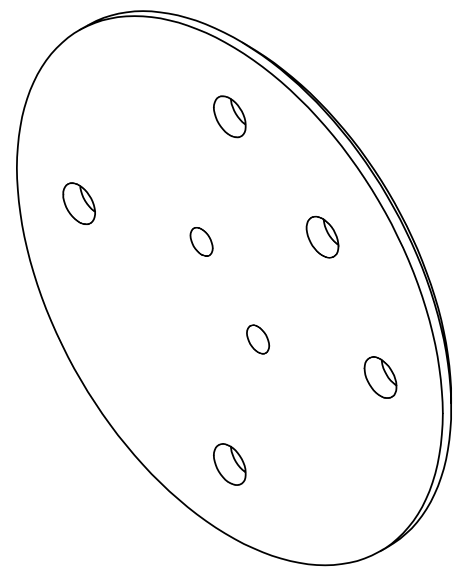

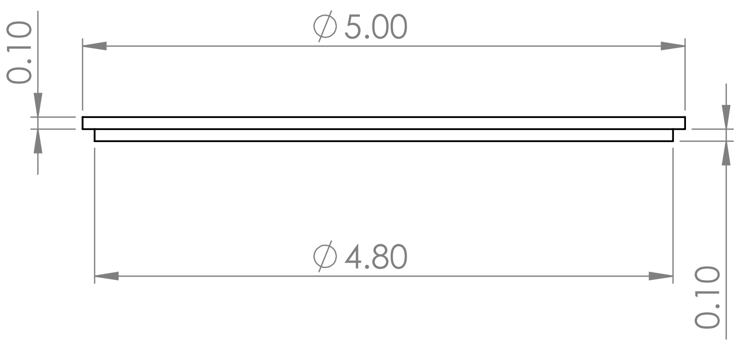

REFERENCE FILE:	Bottom_Plate_CF			QUANTITY 1
ENGLISH DIMENSIONS IN INCHES	SCALE: 2:3	DRAWN BY Julien Otis-L	DATE 12/05/2019	APPROVED Isabelle P-A
GENERAL TOLERANCES 1 DECIMAL ±0.1 2 DECIMAL ±0.01 3 DECIMAL ±0.002		3480 UNIVERSITY ST. MONTREAL, QC, H3A 0E9 CANADA www.mcgillrocketteam.com		
SURFACE TEXTURE		MODEL NAME Bottom Plate		
MATERIAL Carbon Fiber		DRAWING NO. 1		SHEET 1 OF 1

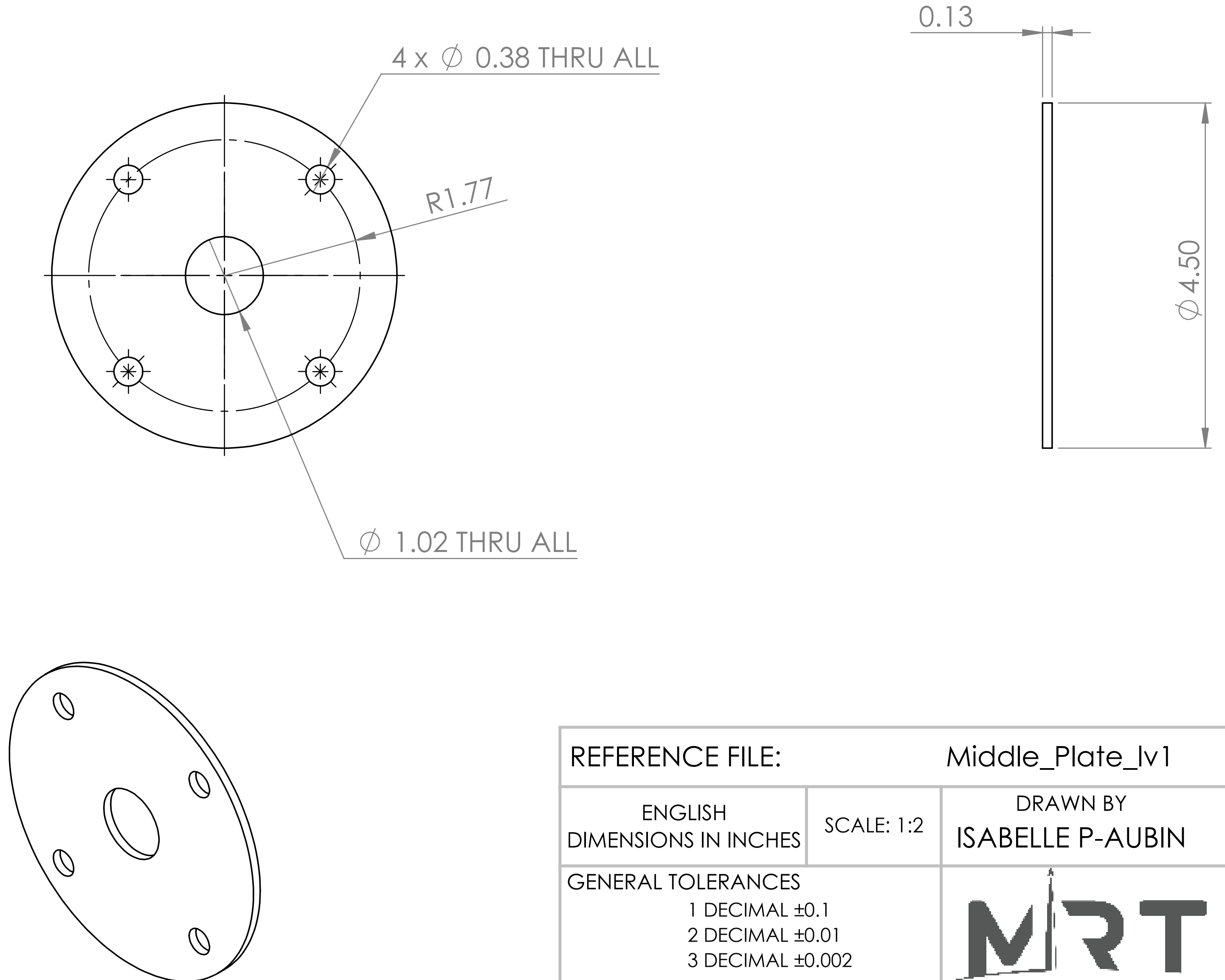

REFERENCE FILE:		Middle_Plate_lv1		QUANTITY 1
ENGLISH DIMENSIONS IN INCHES	SCALE: 1:2	DRAWN BY ISABELLE P-AUBIN	DATE 12.05.2019	APPROVED CR 13.05.2019
GENERAL TOLERANCES 1 DECIMAL ±0.1 2 DECIMAL ±0.01 3 DECIMAL ±0.002		MRT	3480 UNIVERSITY ST. MONTREAL, QC, H3A 0E9 CANADA www.mcgillrocketteam.com	
SURFACE TEXTURE		MODEL NAME Payload Middle Plate		
MATERIAL Al 6061 T6		DRAWING NO. 5		SHEET 1 OF 1

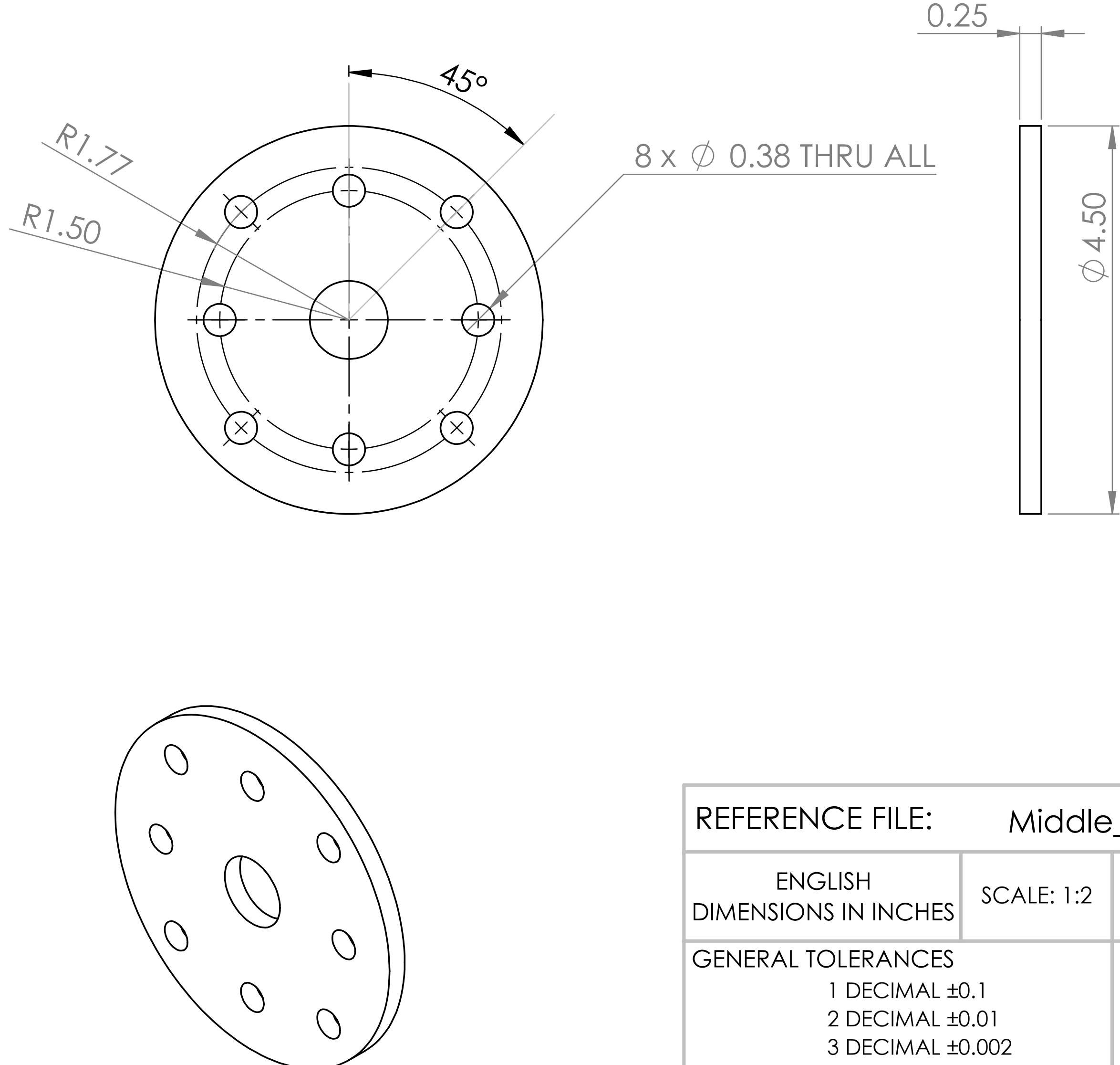

REFERENCE FILE:	Middle_Plate_lv2			QUANTITY 1
ENGLISH DIMENSIONS IN INCHES	SCALE: 1:2	DRAWN BY ISABELLE P-AUBIN	DATE 12.05.2019	APPROVED CR 13.05.2019
GENERAL TOLERANCES 1 DECIMAL ±0.1 2 DECIMAL ±0.01 3 DECIMAL ±0.002		MRT	3480 UNIVERSITY ST. MONTREAL, QC, H3A 0E9 CANADA www.mcgillrocketteam.com	
SURFACE TEXTURE		MODEL NAME Payload Middle Plate 2		
MATERIAL Al 6061 T6		DRAWING NO. 7		SHEET 1 OF 1

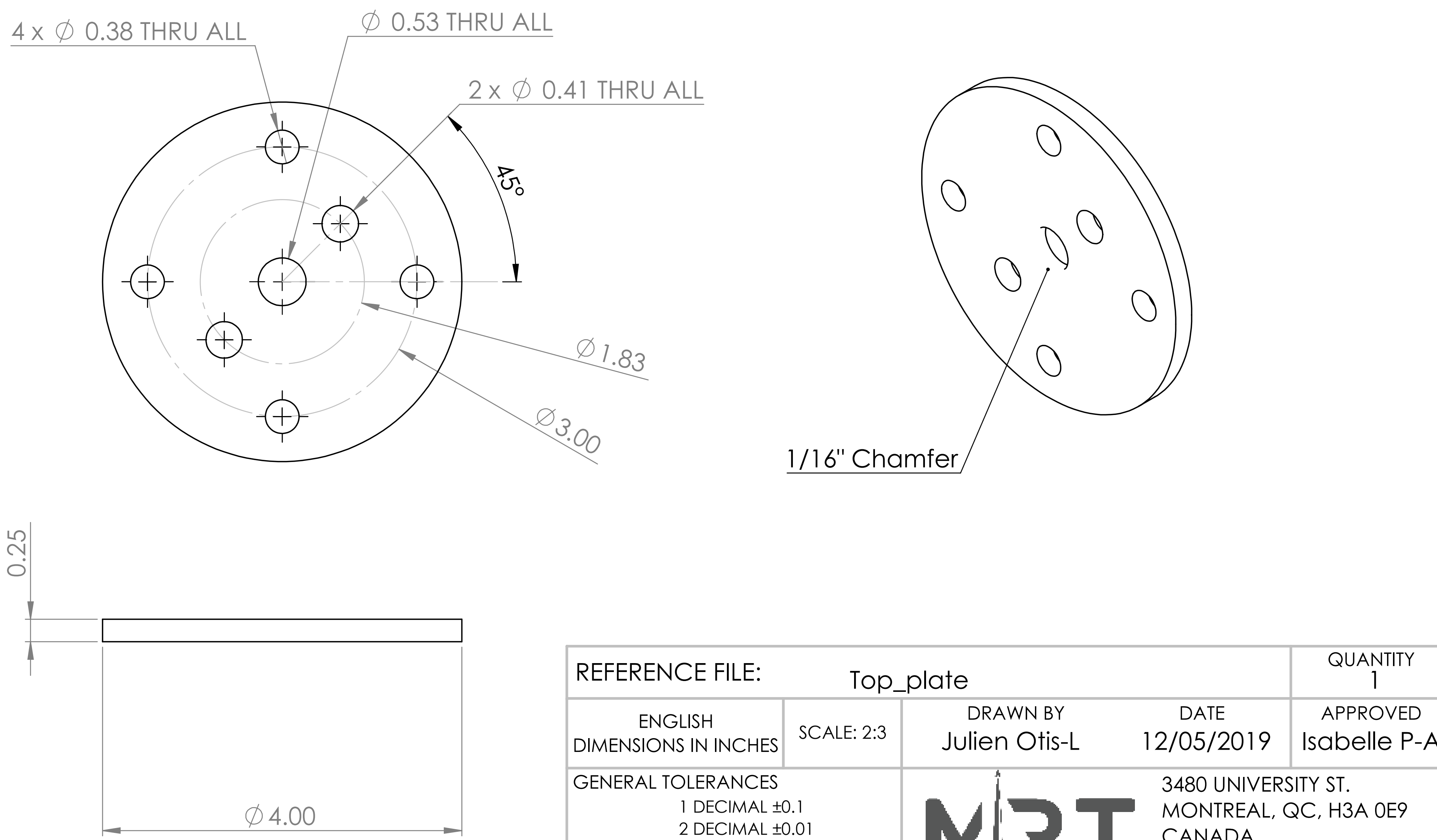

REFERENCE FILE: Top_plate				QUANTITY 1
ENGLISH DIMENSIONS IN INCHES	SCALE: 2:3	DRAWN BY Julien Otis-L	DATE 12/05/2019	APPROVED Isabelle P-A
GENERAL TOLERANCES 1 DECIMAL ±0.1 2 DECIMAL ±0.01 3 DECIMAL ±0.002		MRT	3480 UNIVERSITY ST. MONTREAL, QC, H3A 0E9 CANADA www.mcgillrocketteam.com	
SURFACE TEXTURE		MODEL NAME Top Plate		
MATERIAL 1045 Steel		DRAWING NO. 9		SHEET 1 OF 1

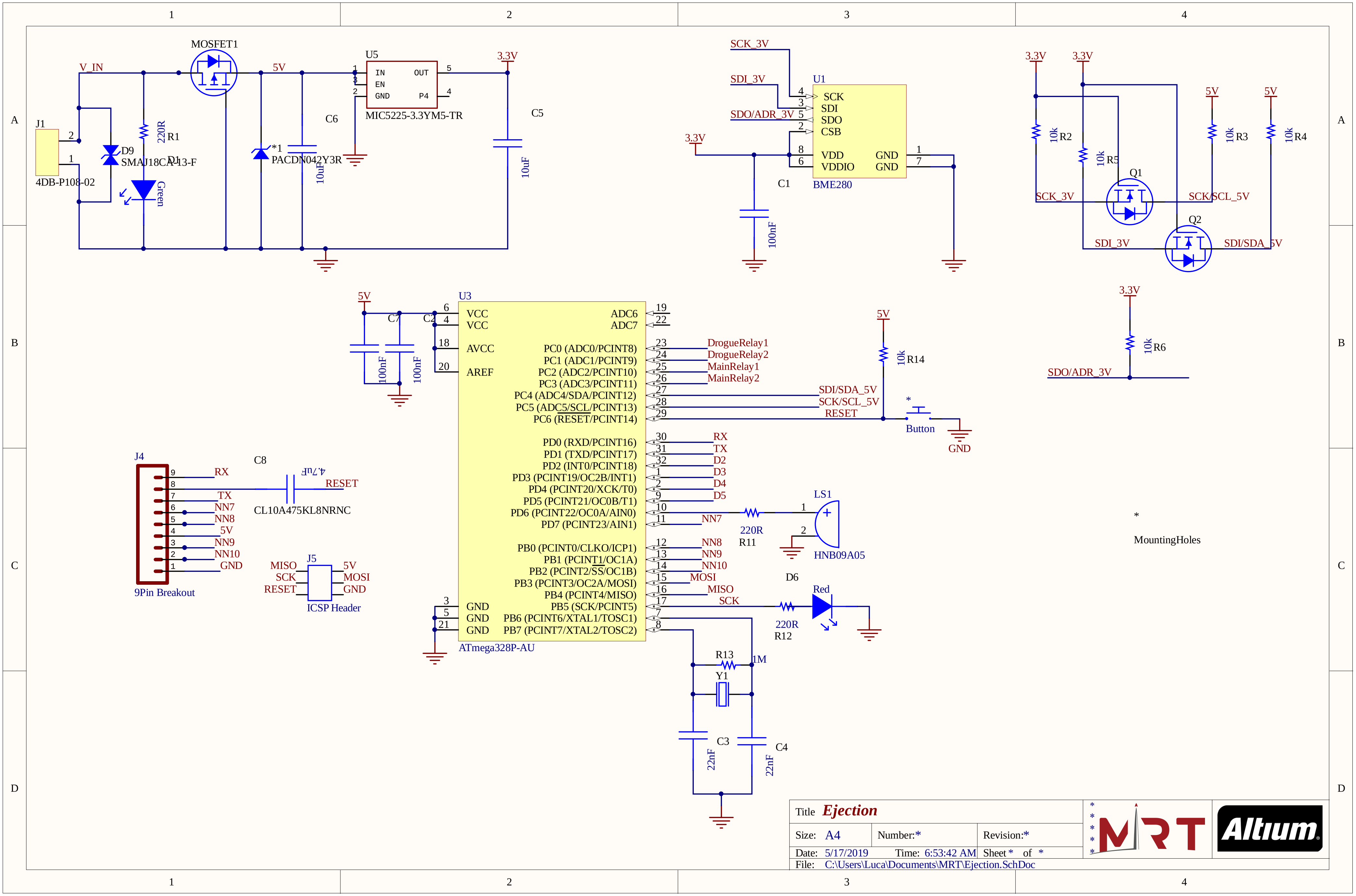

V_IN
J1
4DB-P108-02
D9
SMAJ18CA-13-F
D1
Green
R1
220R
MOSFET1
5V
*1
PACDN042Y3R
C6
10uF
U5
IN
EN
GND
OUT
P4
MIC5225-3.3YM5-TR
3.3V
C5
10uF
SCK_3V
SDI_3V
SDO/ADR_3V
U1
SCK
SDI
SDO
CSB
VDD
VDDIO
GND
GND
BME280
C1
100nF
R2
R3
R4
R5
10k
5V
Q1
Q2
SCK_3V
SCK/SCL_5V
SDI_3V
SDI/SDA_5V
R6
SDO/ADR_3V
U3
VCC
VCC
AVCC
AREF
ADC6
ADC7
PC0 (ADC0/PCINT8)
PC1 (ADC1/PCINT9)
PC2 (ADC2/PCINT10)
PC3 (ADC3/PCINT11)
PC4 (ADC4/SDA/PCINT12)
PC5 (ADC5/SCL/PCINT13)
PC6 (RESET/PCINT14)
PD0 (RXD/PCINT16)
PD1 (TXD/PCINT17)
PD2 (INT0/PCINT18)
PD3 (PCINT19/OC2B/INT1)
PD4 (PCINT20/XCK/T0)
PD5 (PCINT21/OC0B/T1)
PD6 (PCINT22/OC0A/AIN0)
PD7 (PCINT23/AIN1)
PB0 (PCINT0/CLKO/ICP1)
PB1 (PCINT1/OC1A)
PB2 (PCINT2/SS/OC1B)
PB3 (PCINT3/OC2A/MOSI)
PB4 (PCINT4/MISO)
PB5 (SCK/PCINT5)
PB6 (PCINT6/XTAL1/TOSC1)
PB7 (PCINT7/XTAL2/TOSC2)
GND
GND
GND
ATmega328P-AU
C7
C2
100nF
100nF
DrogueRelay1
DrogueRelay2
MainRelay1
MainRelay2
SDI/SDA_5V
SCK/SCL_5V
RESET
R14
10k
Button
GND
RX
TX
D2
D3
D4
D5
NN7
R11
220R
LS1
HNB09A05
NN8
NN9
NN10
MOSI
MISO
SCK
D6
Red
R12
220R
R13
1M
Y1
C3
22nF
C4
22nF
J4
9Pin Breakout
RX
TX
NN7
NN8
5V
NN9
NN10
GND
C8
4.7uF
RESET
CL10A475KL8NRNC
J5
MISO
SCK
RESET
5V
MOSI
GND
ICSP Header
MountingHoles
Title Ejection
Size: A4
Number:*
Revision:*
Date: 5/17/2019
Time: 6:53:42 AM
Sheet * of *
File: C:\Users\Luca\Documents\MRT\Ejection.SchDoc

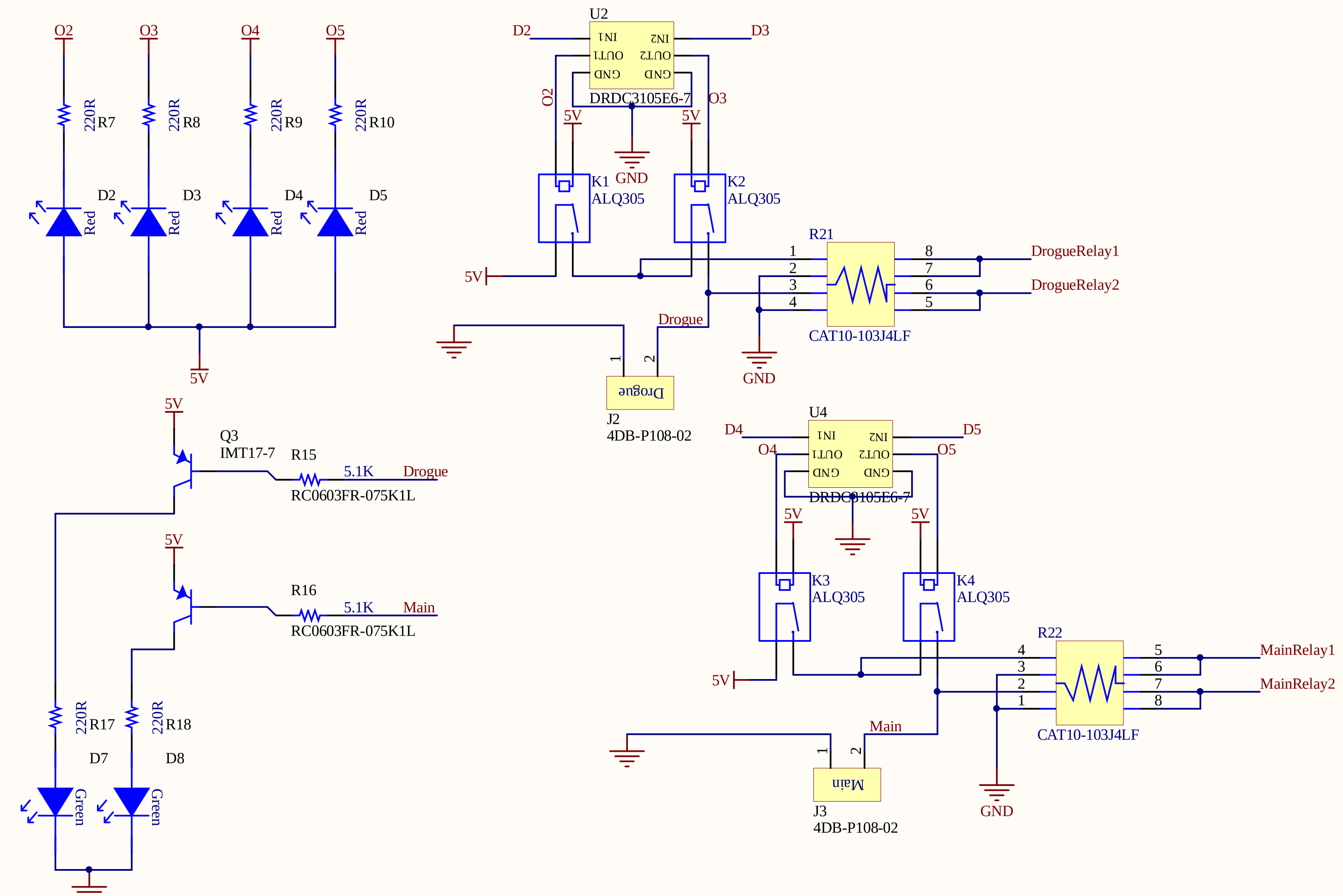

Title **Ematch**		
Size: Letter	Number: *	Revision: *
Date: 5/17/2019	Time: 6:53:15 AM	Sheet * of *
File: C:\Users\Luca\Documents\MRT\Ematch.SchDoc		

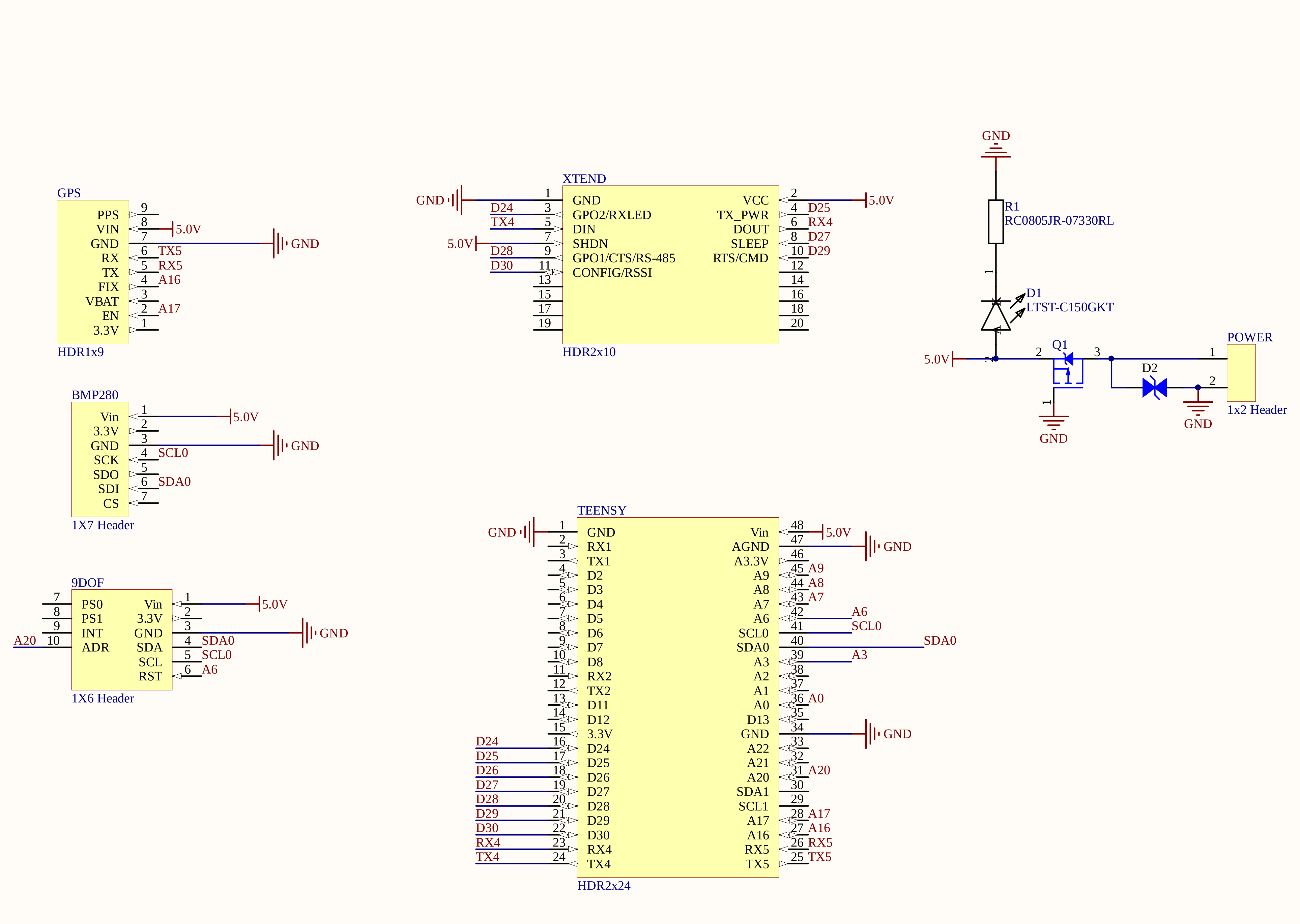

Title	***Telemetry***		
Size: A	Number: *		Revision: *
Date: 5/17/2019	Time: 6:39:24 AM	Sheet * of *	
File: C:\Users\Luca\Documents\Altium\MRT_2019_Telemetry_Breakout\Telemetry.SchDoc			

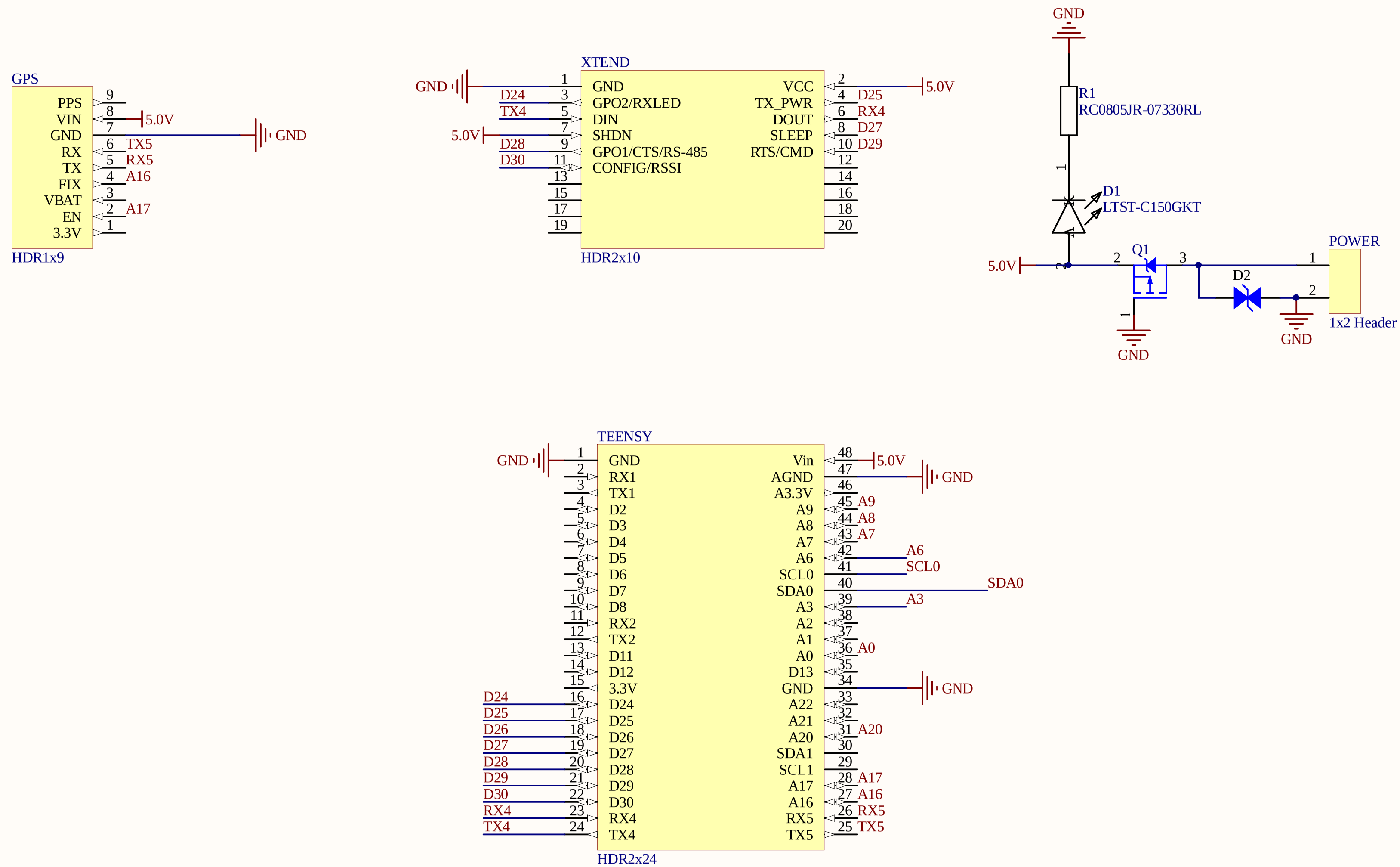

Title: **GPS Redundancy**		
Size: Letter	Number:*	Revision:*
Date: 5/17/2019	Time: 7:00:31 AM	Sheet* of *
File: C:\Users\Luca\Documents\Altium\MRT_2019_GPS_Redundancy\Telemetry.SchDoc		

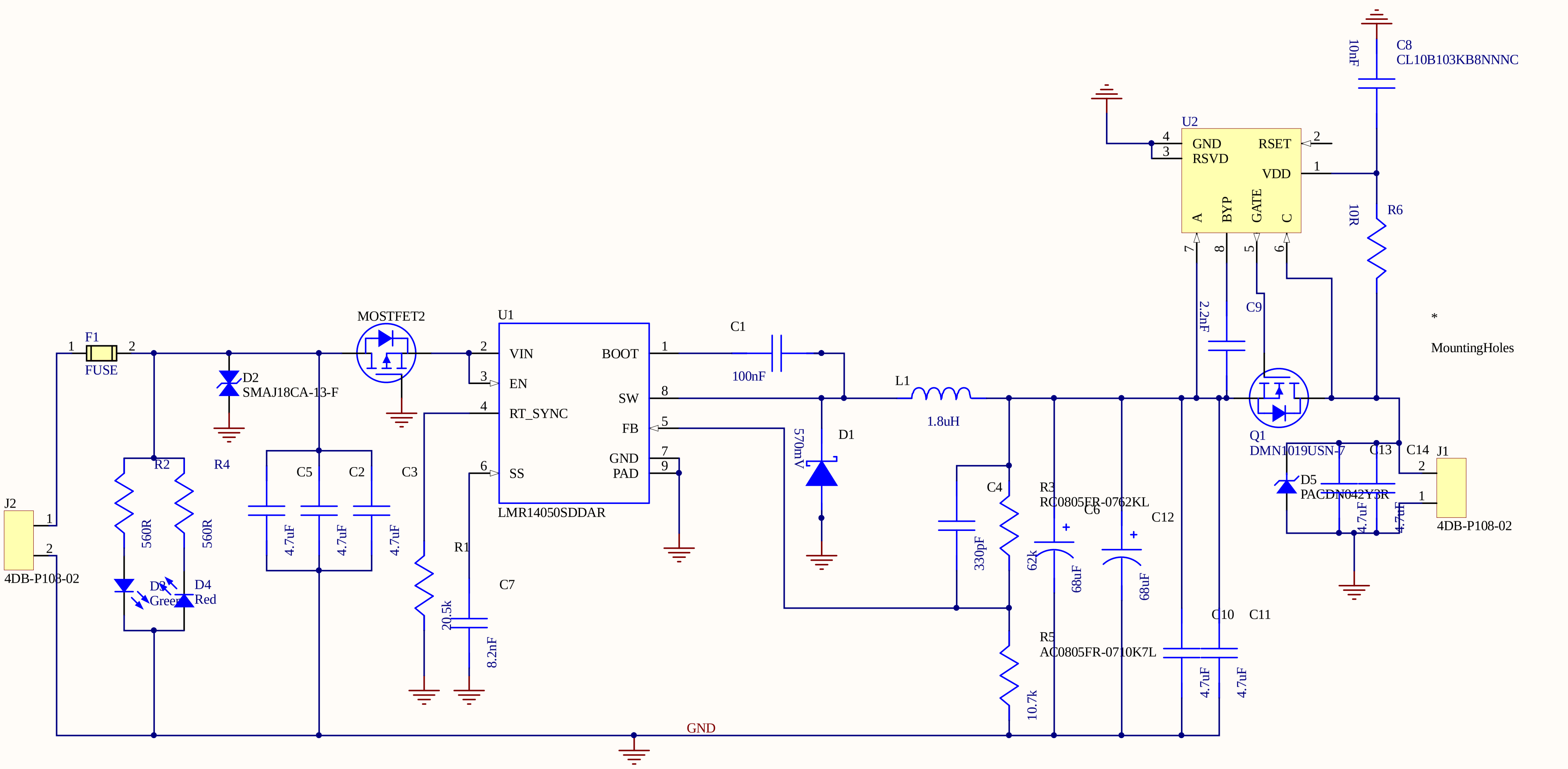

Title	Power Management		
Size: Letter	Number: *		Revision: *
Date: 5/17/2019	Time: 6:54:01 AM	Sheet 1 of 1	
File: C:\Users\Luca\Documents\MRT\PowerManagementNewComponents.schdoc			

Acknowledgments

The team would like to acknowledge the financial and material support of our many sponsors, too numerous to list here, as well as the assistance and feedback from many advisors: Michel Wander from the Canadian Space Agency, Yves Dufour from the Quebec Rocketry Club, Tho Le-Ngoc, Robert Morawski and Harry H. Lee from the Communications Lab, Ken Dewar, Caroline Monat and Benoit Cousineau from MI4 and many others. We would also like to thank the Department of Chemical Engineering for providing us with a working space to manufacture most of our airframe, at a time when we were questioning our ability to complete this project. Specifically, a large thank you to Viviane Yargeau, Richard Leask, Ranjan Roy and Andrew Golsztajn. Additionally, a big thank you to the McGill technicians Mathieu Beauchesne, Lydia Dyda, Harry Harihar and Andy Hofmann for their invaluable help year after year. Thank you as well to our friends and family members for their constant and unwavering support, and to all ESRA staff and judges for the countless hours they put into organizing this incredible competition.

The team would finally like to thank Bertrand (Figure 47), our team betta fish, for always being there for us.

Fig. 47 Team Fish Bertrand

References

[1] Clancy, L. J., *Aerodynamics*, Halsted Press, 1975.

[2] Cho, J., and Chang, Y., "Supersonic flutter analysis of wings using an unsteady 3D panel method," *Computers & fluids*, Vol. 30, No. 2, 2001, pp. 237–256.

[3] Lesage, J., Papais, S., et al., "Team 93 Technical Report: Project Stella II," *SAC 2018 Technical Reports*, 2018.

[4] Online, W. W., "Truth Or Consequences, New Mexico, United States of America Historical Weather Almanac," , May 2019. URL `https://www.worldweatheronline.com/truth-or-consequences-weather-history/new-mexico/us.aspx`.